

Impact of SiC and RC-IGBT on Electric Railway and EV Drives

Nov. 2nd, 2019

Dr. T. Fujihira (藤平 龍彦)

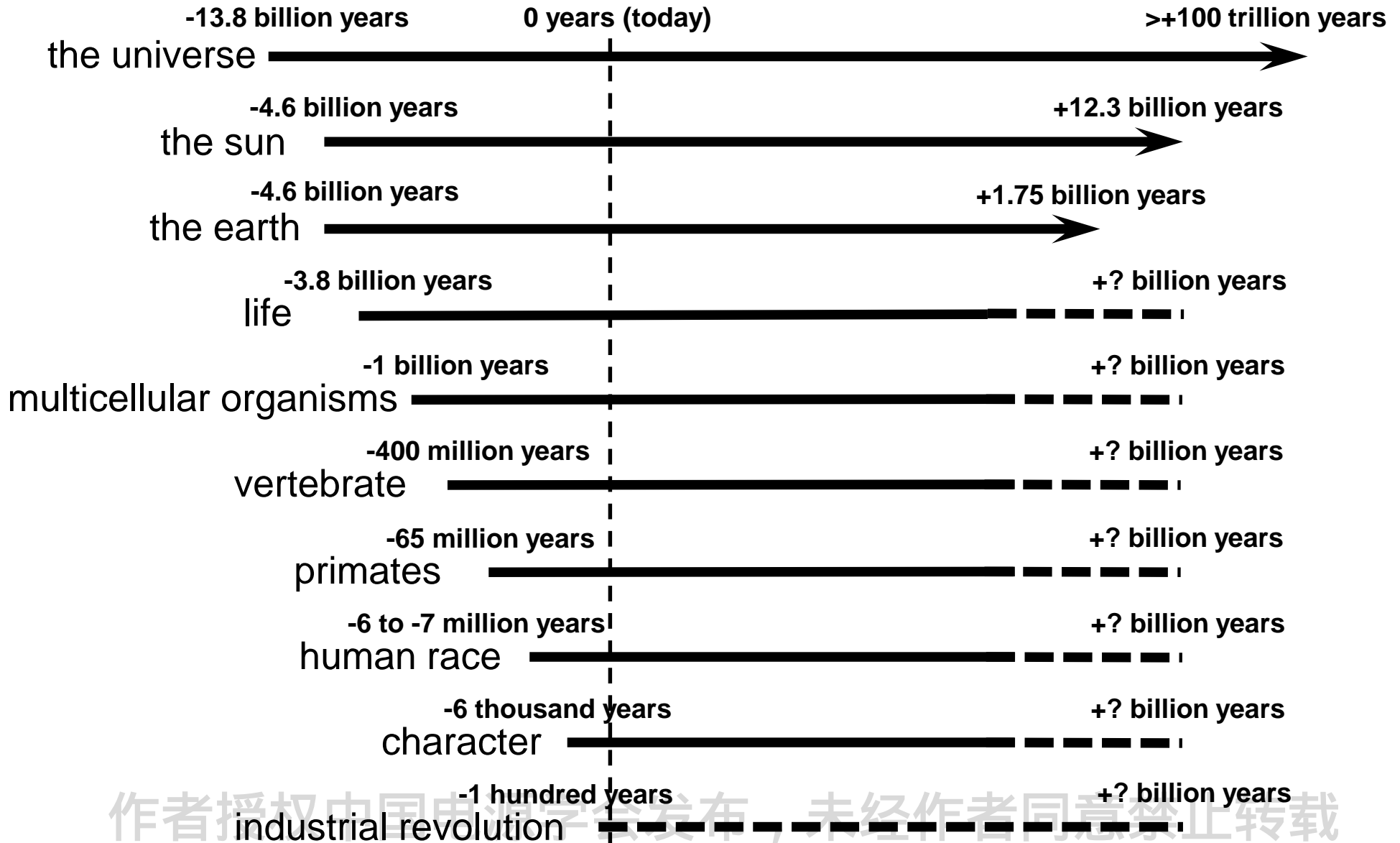
Fuji Electric Co., Ltd (富士電機)

作者授权中国电源学会发布，未经作者同意禁止转载

- Introduction
- RC-IGBT for xEV
- SiC-MOSFET
- Advanced SiC Devices
- Conclusions

作者授权中国电源学会发布，未经作者同意禁止转载

Past, Future, and Today



作者授权中国电机学会发布，未经作者同意禁止转载

12 Risks that Threaten Human Civilization



Extreme Climate Change



Nuclear War



Global Pandemic

□ Extreme Climate Change

□ Nuclear War

□ Global Pandemic

□ ...



Ecological Catastrophe



Global System Collapse



Major Asteroid Impact



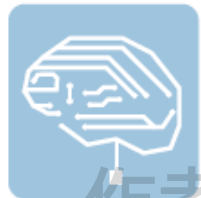
Super-volcano



Synthetic Biology



Nanotechnology



Artificial Intelligence



Unknown Consequences



Future Bad Global Governance

Current risk



5 key factors:

- 1 The uncertainties in climate sensitivity models, including the tail.
- 2 The likelihood - or not - of global coordination on controlling emissions.
- 3 The future uptake of low carbon economies, including energy, mobility and food systems.
- 4 Whether technological innovations will improve or worsen the situation, and by how much.
- 5 The long-term climate impact caused by global warming.

Dennis Pamlin
Executive Project Manager Global Risks
Global Challenges Foundation

dennis@globalchallenges.org
globalchallenges.org

or

Stuart Armstrong
James Martin Research Fellow
Future of Humanity Institute
Oxford Martin School
University of Oxford

stuart.armstrong@philosophy.ox.ac.uk
fhi.ox.ac.uk

作者授权中国电源学会发布，Source: 12 Risks that threaten human civilization
Global Challenges Foundation, Feb. 2015

Resolution of UNs 70th General Assembly

Resolution adopted by the General Assembly on 25 September 2015

[without reference to a Main Committee (A/70/L.1)]

70/1. Transforming our world: the 2030 Agenda for Sustainable Development



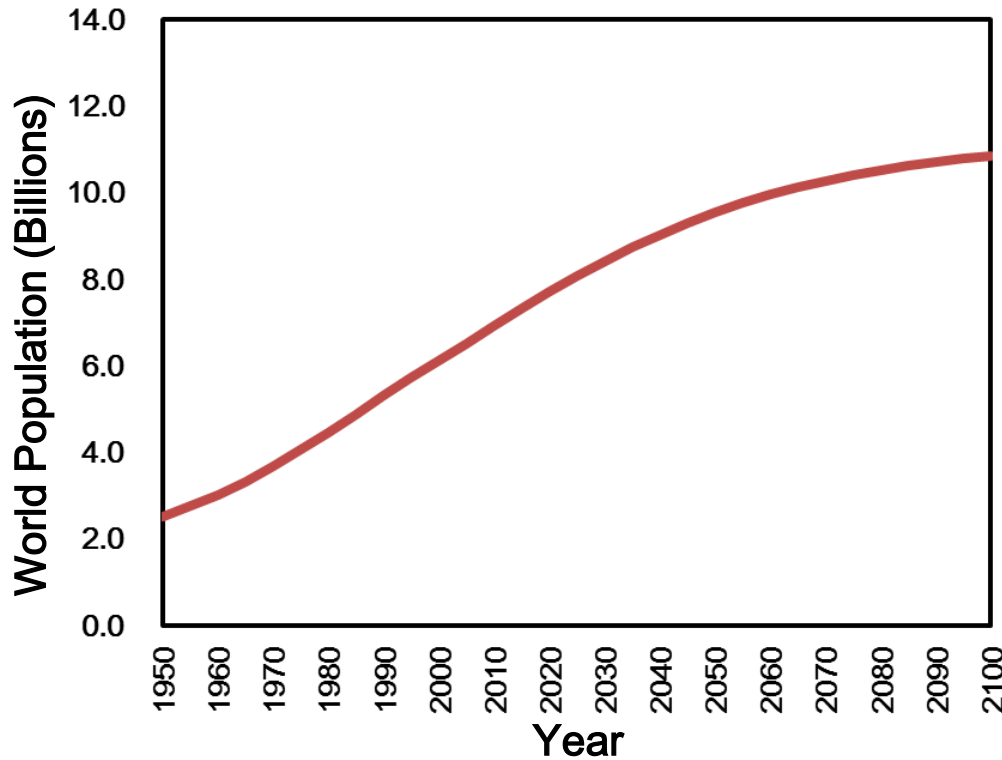
SUSTAINABLE DEVELOPMENT GOALS

17 GOALS TO TRANSFORM OUR WORLD



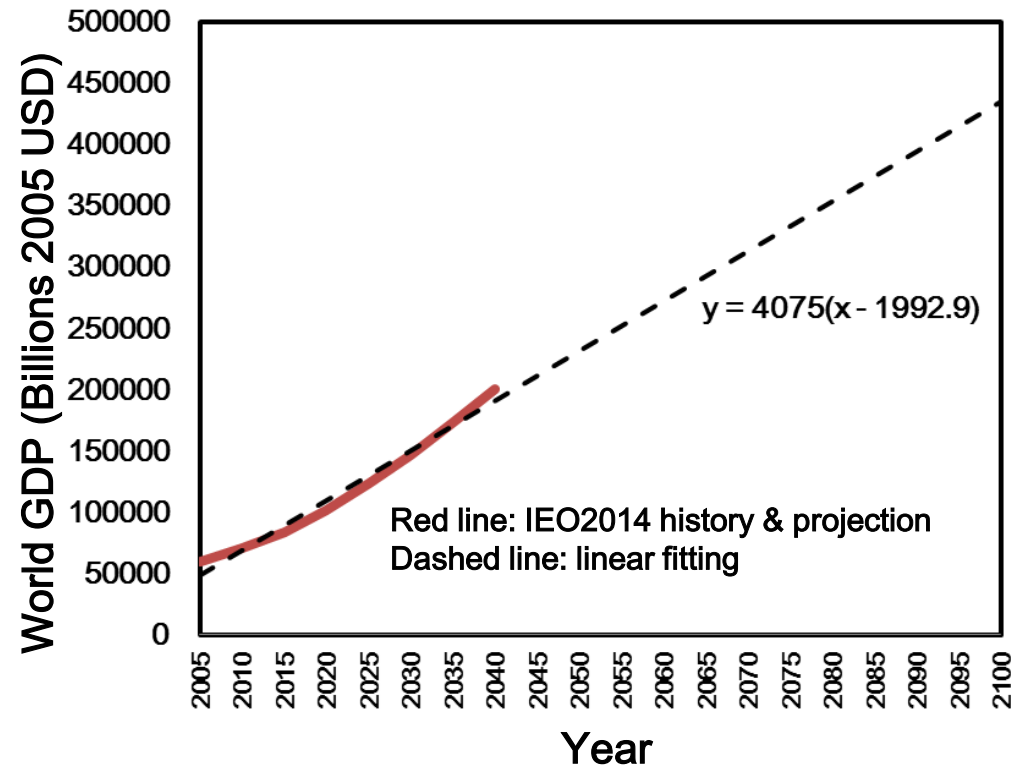
What will come in this century?

□ Population grows 1.5 times



Source: World Population Prospects: The 2012 Revision
Population Division of the Department of Economic
and Social Affairs of the United Nations Secretariat

□ GDP more than 4.5 times



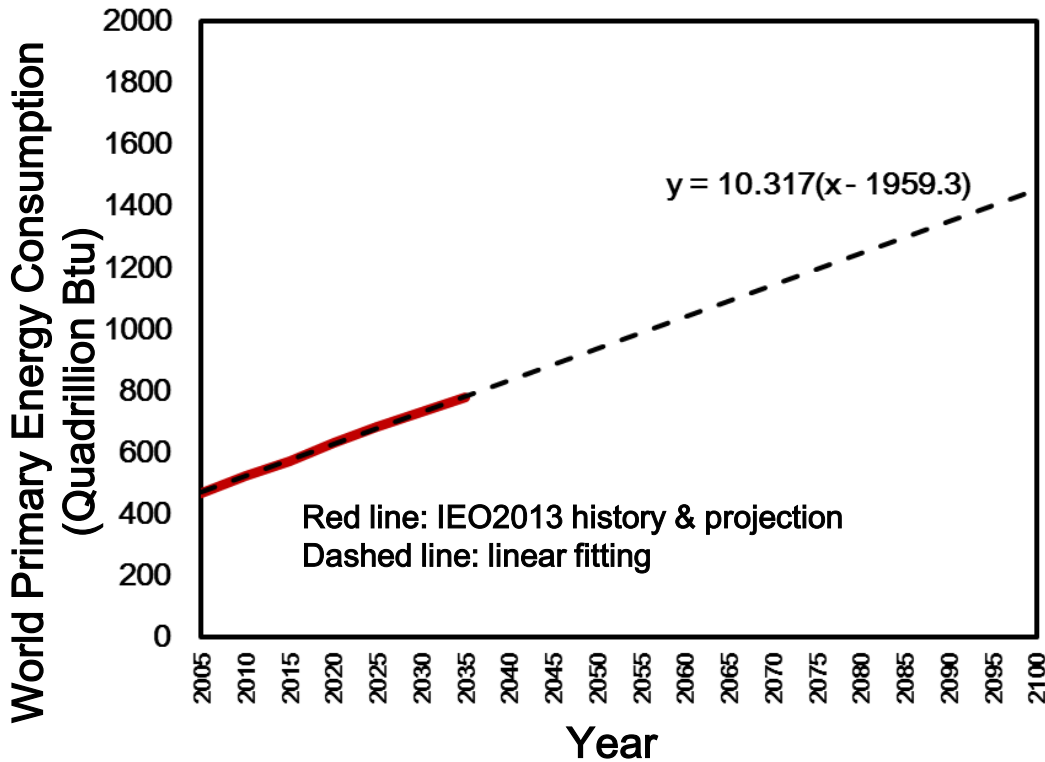
Source: International Energy Outlook 2014, Reference case,
U.S. Energy Information Administration

作者授权中国电源学会发布，未经作者同意禁止转载

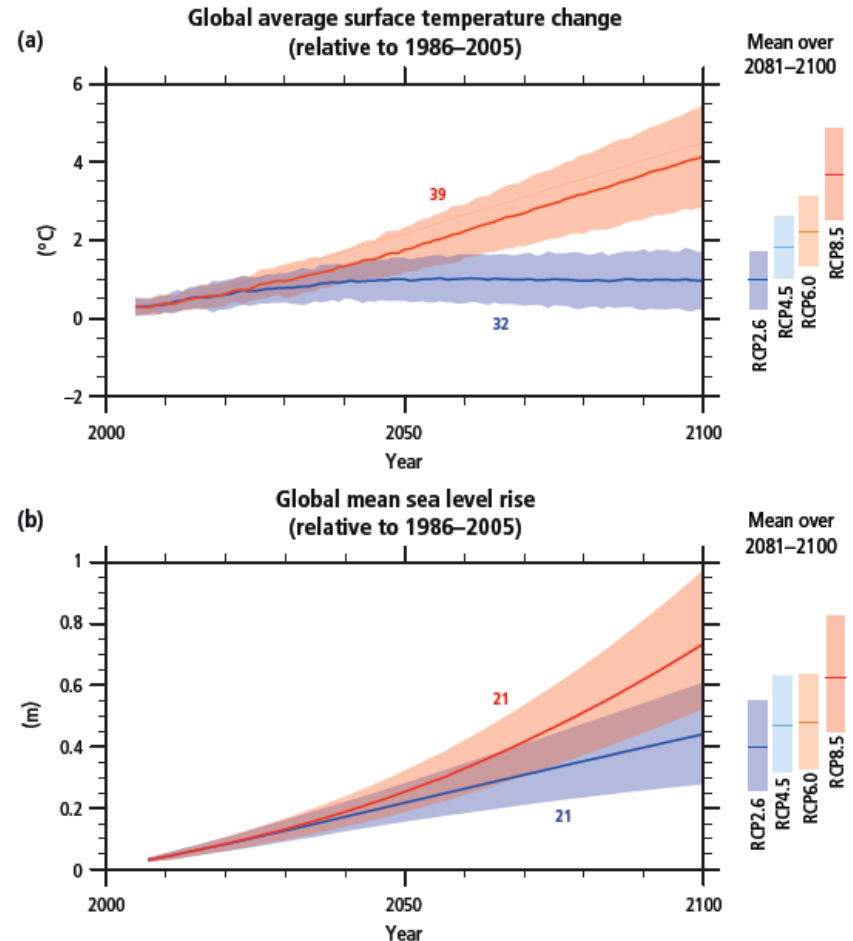
□ Energy consumption 2.5 times

□ Temperature rise 1-4 degree

□ Sea level rise 0.4-0.8 meter



Source: International Energy Outlook 2013, Reference case, U.S. Energy Information Administration

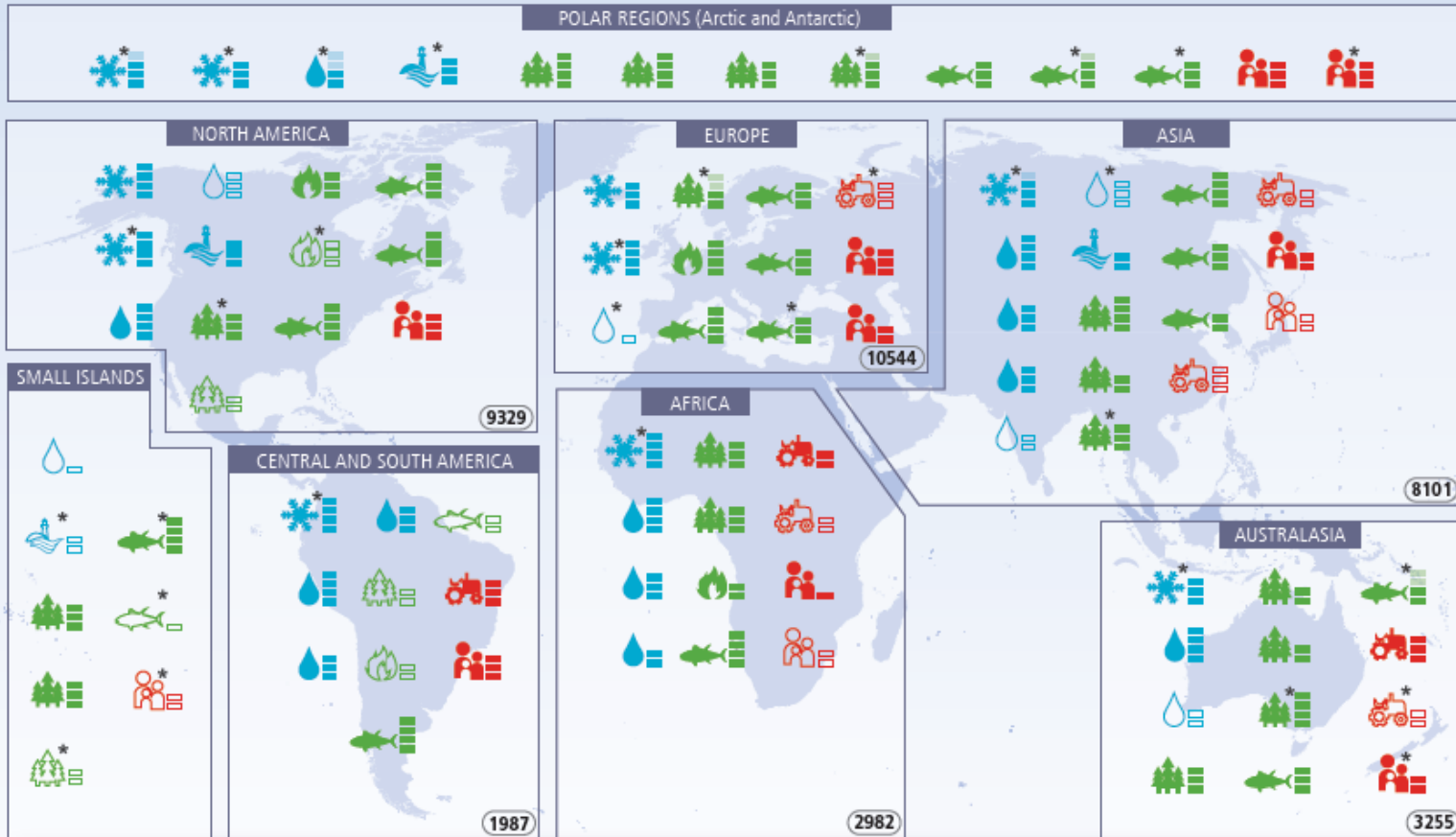


Source: IPCC 5th Assessment Report
Climate Change 2014 Synthesis Report, 2015
Figure SPM.6.

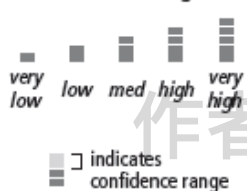
作者授权中国电源学会发布，未经许可禁止转载

Widespread Impacts of Climate Change

Widespread impacts attributed to climate change based on the available scientific literature since the AR4



Confidence in attribution to climate change



Observed impacts attributed to climate change for

Physical systems

- Glaciers, snow, ice and/or permafrost
- Rivers, lakes, floods and/or drought
- Coastal erosion and/or sea level effects

Biological systems

- Terrestrial ecosystems
- Wildfire
- Marine ecosystems

Human and managed systems

- Food production
- Livelihoods, health and/or economics

* Impacts identified based on availability of studies across a region

Outlined symbols = Minor contribution of climate change
Filled symbols = Major contribution of climate change

Source:
IPCC 5th Assessment Report
Climate Change 2014 Synthesis
Report, 2015.
Figure SPM.4.



United Nations

FCCC/CP/2015/10/Add.1



Framework Convention on
Climate Change

Distr.: General
29 January 2016

Original: English

Conference of the Parties

Report of the Conference of the Parties on its twenty-first session, held in Paris from 30 November to 13 December 2015

Addendum

Part two: Action taken by the Conference of the Parties at its twenty-first session

Contents

Decisions adopted by the Conference of the Parties

Emphasizing with serious concern the urgent need to address the significant gap between the aggregate effect of Parties' mitigation pledges in terms of global annual emissions of greenhouse gases by 2020 and aggregate emission pathways consistent with holding the increase in the global average temperature to well below 2 °C above pre-industrial levels and pursuing efforts to limit the temperature increase to 1.5 °C above pre-industrial levels,

What we should do

as power electronic R&D or industries are

- ❑ switch from fossil to renewable energies
- ❑ shift from car, jet, and combustion engines to xEV and electric transportations
- ❑ increase efficiency of power generation, transmission, and conversion
- ❑ reduce consumption, increase reuse and recycle of limited natural resources including Cu and Iron in power electronic systems

to establish a sustainable society

作者授权中国电源学会发布，未经作者同意禁止转载

“The eyes of all future generations are upon you.”

"And if you choose to fail us, I say: We will never forgive you. We will not let you get away with this. Right here, right now is where we draw the line. The world is waking up. And change is coming, whether you like it or not." Greta Thunberg told world leaders Sep. 23rd, 2019, speaking at the U.N. Climate Action Summit in New York City.



作者授权中国电源学会，未经作者同意禁止转载

□ RC-IGBT for xEV

作者授权中国电源学会发布，未经作者同意禁止转载

Fuji Electric Contributions to xEV

2 in 1 IPM



Production
Buck boost
converter

Company T : HEV



Module



Production
Inverter



IPM



14 in 1 IPM



Production
2 Inverters
with buck boost
converter

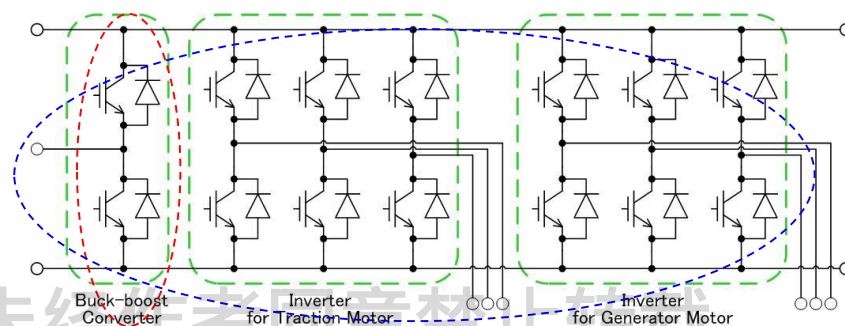
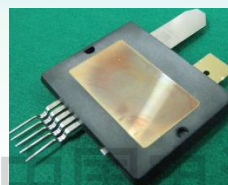
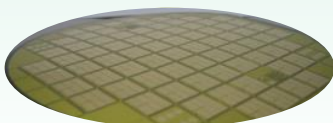
Company H : HEV/PHEV



Power chip for double side cooling system

Production
Power chip by Fuji

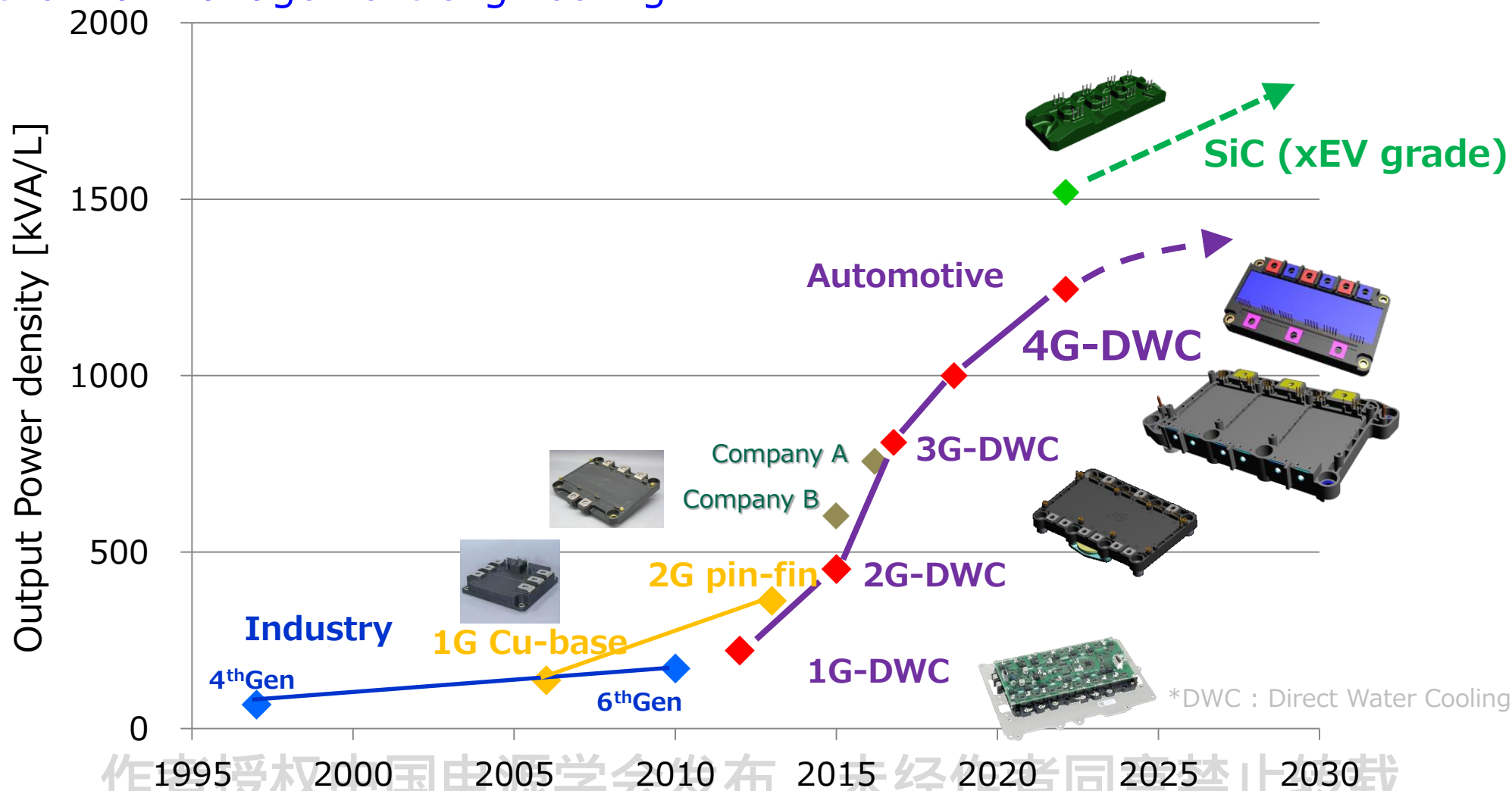
Company D : HEV



作者授权中国电源学会发布，未经作者同意禁止转载

IGBT Module Power Density Trend

Higher power density challenge with the best integration in chip-package-thermal management engineering.



1995 2000 2005 2010 2015 2020 2025 2030

* Output Power density [kVA/L] = Max output power [kVA] / Module volume [L] in continuous

- ❑ Direct water cooling (DWC) aluminum fin
to reduce R_{th} , pressure loss, weight, and thickness
- ❑ RC-IGBT from 3G DWC
to reduce die, DCB, module area and R_{th}
- ❑ Lead-Frame wiring from 4G DWC
to reduce size, L_s , R_{th} , T_{jpeak} , and to increase I^2t

作者授权中国电源学会发布，未经作者同意禁止转载

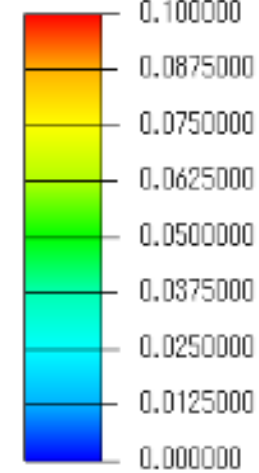
3G DWC: Cooling Performance Improved

1st generation

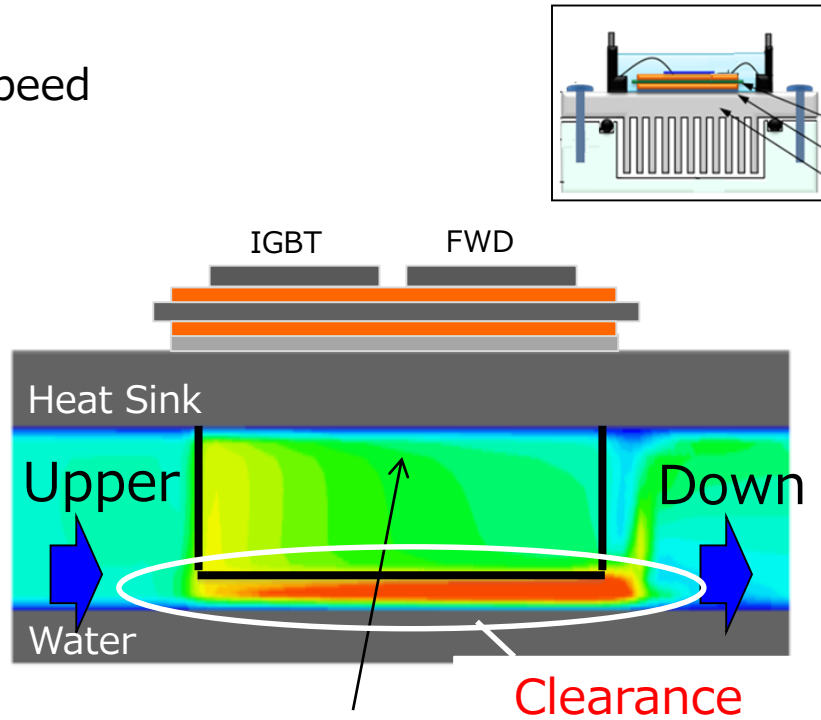
3rd generation

Coolant flows peed

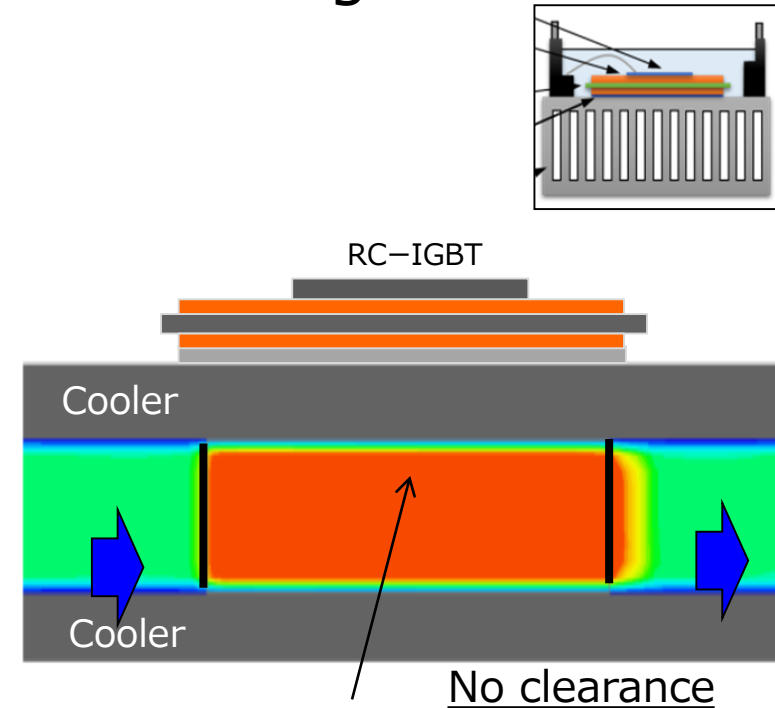
High



Low



Flow speed 0.05m/sec

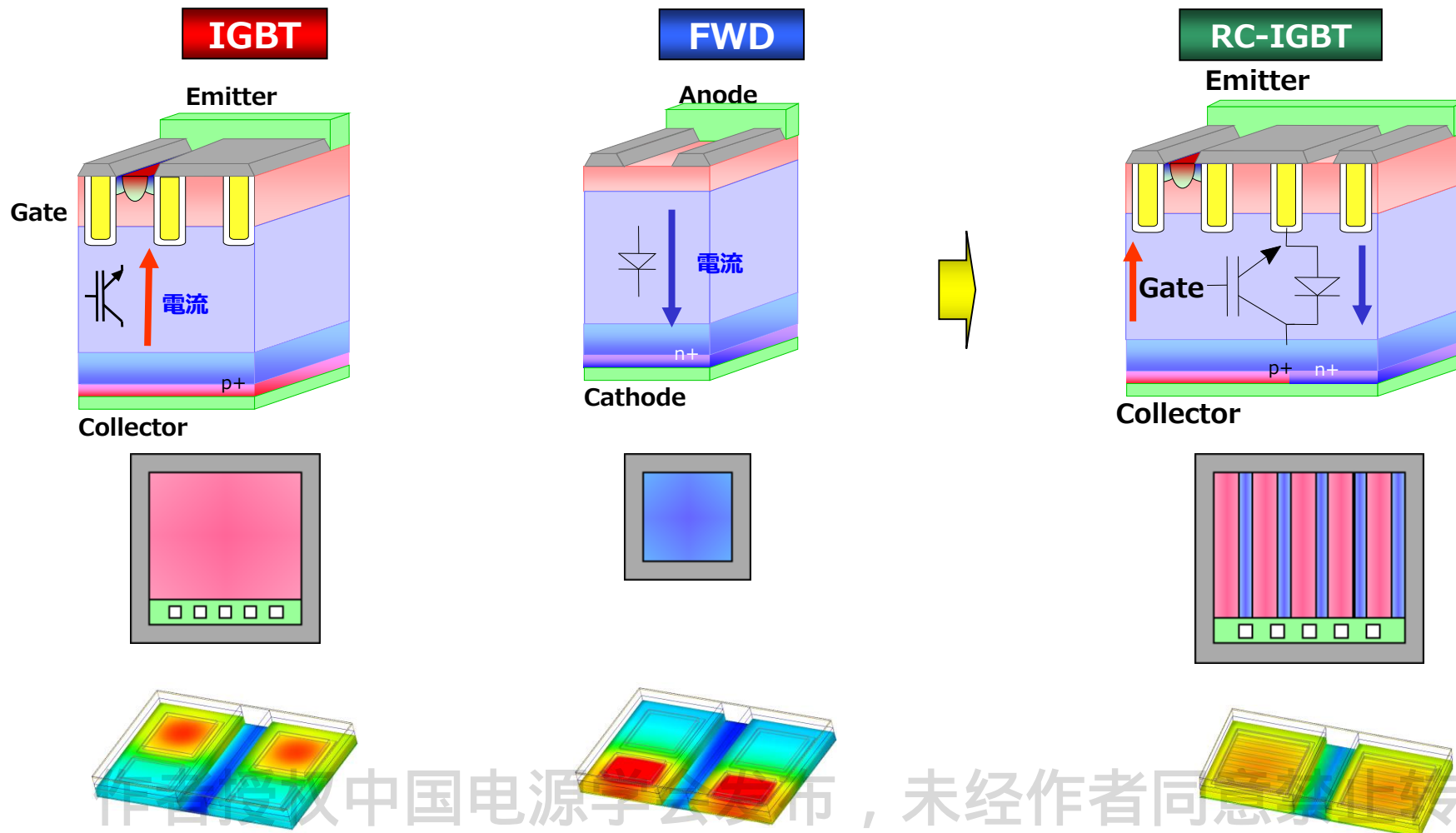


0.1m/sec

■ Coolant flow speed was optimized to flow it near chip area, resulting in **Rth reduction by 30%**.

RC-IGBT from 3G DWC

Monolithic integration of IGBT/FWD,
Additional die shrink available; $R_{thj-c} \downarrow \downarrow$, compact, reduce \$\$\$



中国电源网, 未经作者同意不得转载

RC-IGBT from 3G DWC

Reduction of DCB area by 25%

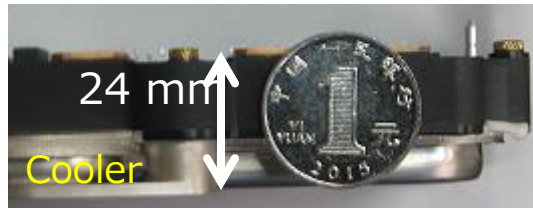
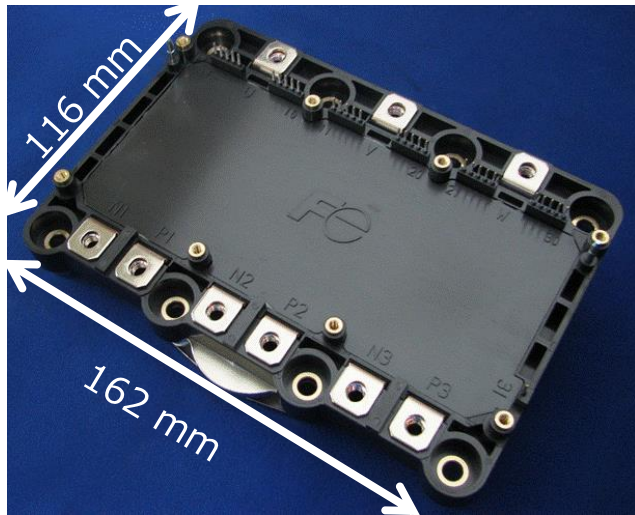
Reduction of parasitic inductance of emitter-to-DCB wiring by 22%

	Conventional IGBT and FWD	Newly developed RC-IGBT
A general Substrate layout of half-bridge circuit		
Ratio of substrate size	1	0.75
Ratio of length between P and N terminal	1	0.78

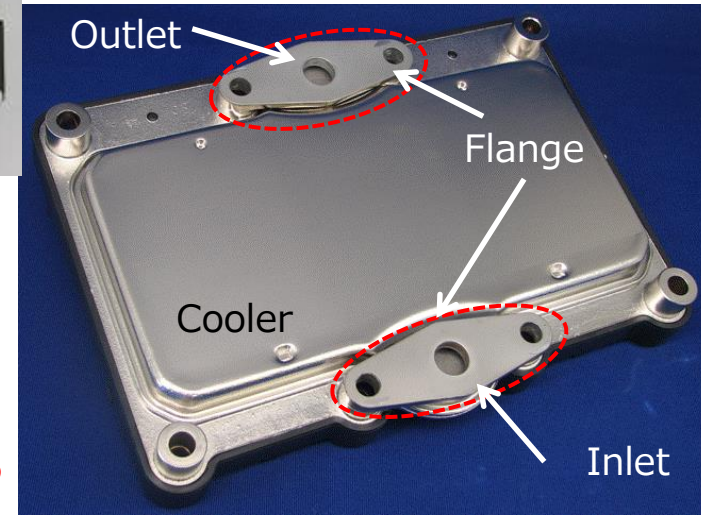
作者授权中国电源学会发布，未经作者同意禁止转载

A general substrate layout of half-bridge circuit.

3G DWC 6in1 RC-IGBT under MP from 2017



Thinner than one RMB coin diameter !!



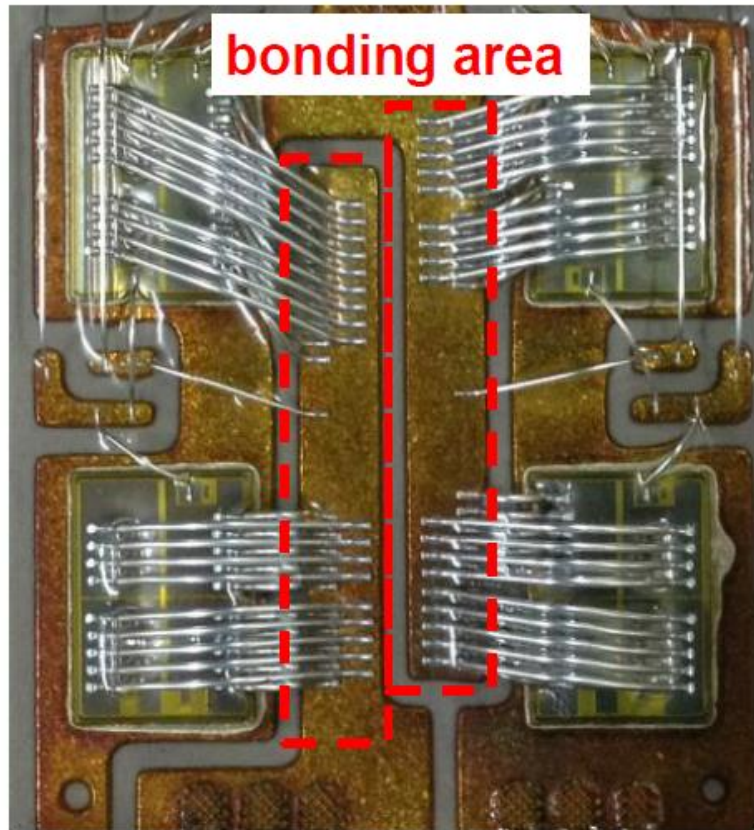
Item	Value
Collector-Emitter voltage	750 V
Implemented Collector current	800 A
Saturation voltage at 175°C	1.65 V
Thermal resistance at 10L/min	0.141 °C/W
Continuous operating junction temperature	175 °C
Size	162×117×24 mm
Weight	570 g
Target to motor output power to be applied	100-150 kW

■ M653 is high power, light-weight, small size and ultra-thin.

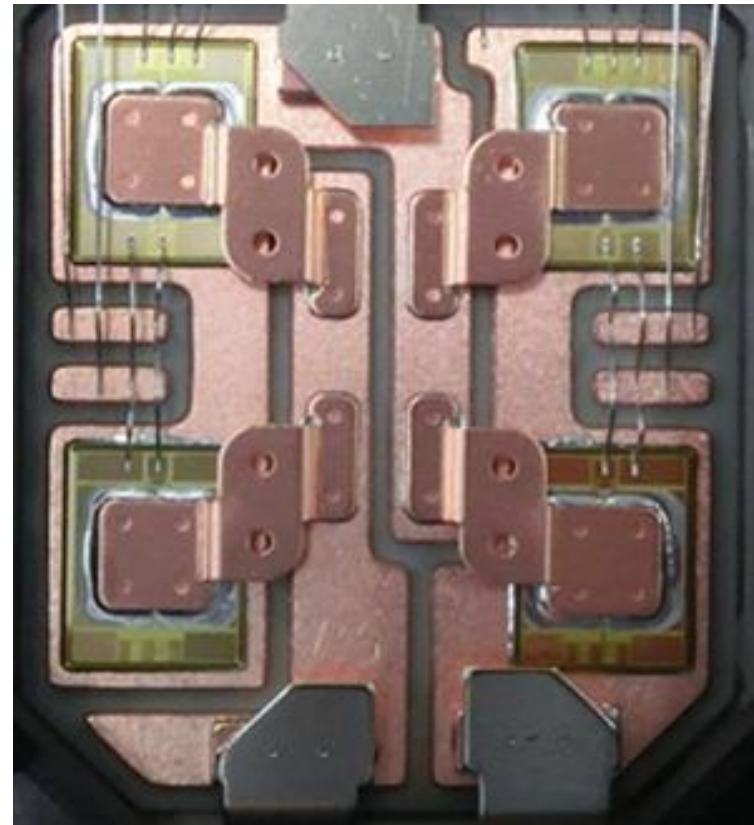
Lead-Frame Wiring from 4G DWC

Support for large current

Reduction of parasitic inductance of emitter-to-DCB



Aluminum-wire-bond wiring

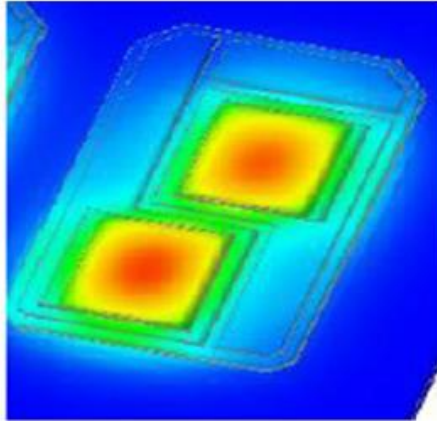


Lead-frame wiring

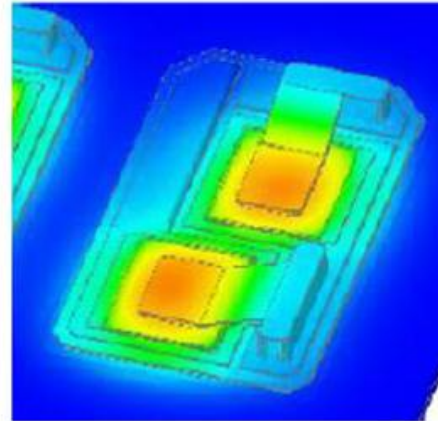
作者授权中国电源学会发布，未经作者同意禁止转载

Lead-Frame Wiring from 4G DWC

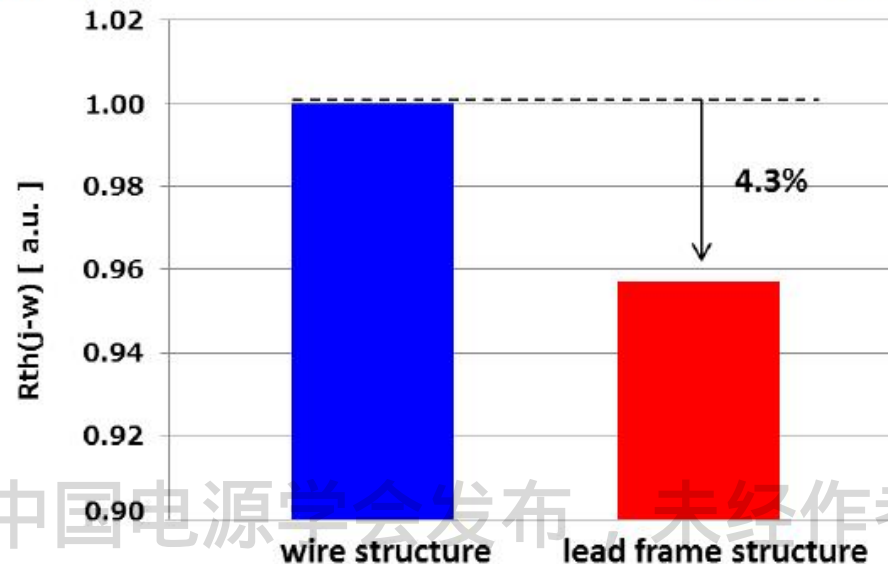
Reduction of R_{th} by 4.3%
Reduction of peak chip-surface temperature



wire structure



lead frame structure



作者授权中国电源学会发布，未经作者同意禁止转载

□ SiC-MOSFET

作者授权中国电源学会发布，未经作者同意禁止转载

Application Examples of SiC Devices

□ Application of SiC is gradually widening, examples at Fuji Electric.

CY2012

2013

2014

2015

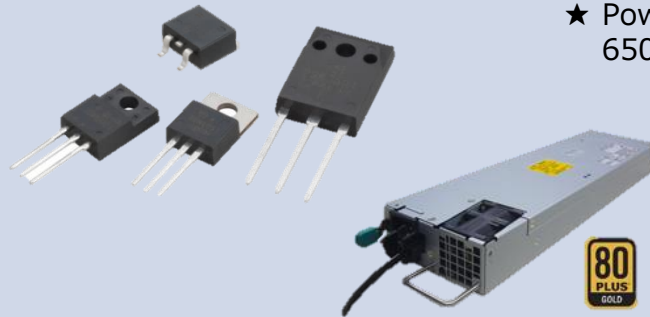
2016

2017

2018

2019

Discrete SiC-SBD



★ Power Supply
650V SiC-SBD

★ EV charger
1200V SiC-SBD



SiC-SBD Hybrid Module

★ General purpose INV
600V,1200V SiC Hybrid Module



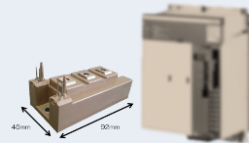
★ Traction propulsion
3300V SiC Hybrid Module



★ UPS
1200V SiC Hybrid Module



★ Servo, Robot
1200V SiC Hybrid Module



★ HEV Racing Car
1200V SiC Hybrid Module

All-SiC Module

★ PCS
1200V All-SiC Module



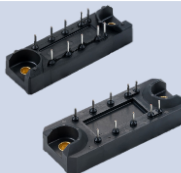
★ Mega solar PCS
1200V All-SiC Module



★ IP6x INV
1200V Trench All-SiC Module



☆ Premium INV
☆ APS and Inverter for traction
1200V Trench All-SiC Module



❑ Loss reduction removed cooling fans, and thus realized environment-resistant, maintenance-free inverters.

Features

- ◆ Best use of low loss and high temperature operation in SiC devices
 - All closed self-cooling structure, as well as downsizing
 - Outdoor installation, application for environment with corrosive gases

400V/37kW



SCF2017 SYSTEM CONTROL FAIR 計測展2017 TOKYO

富士電機 Innovating Energy Technology

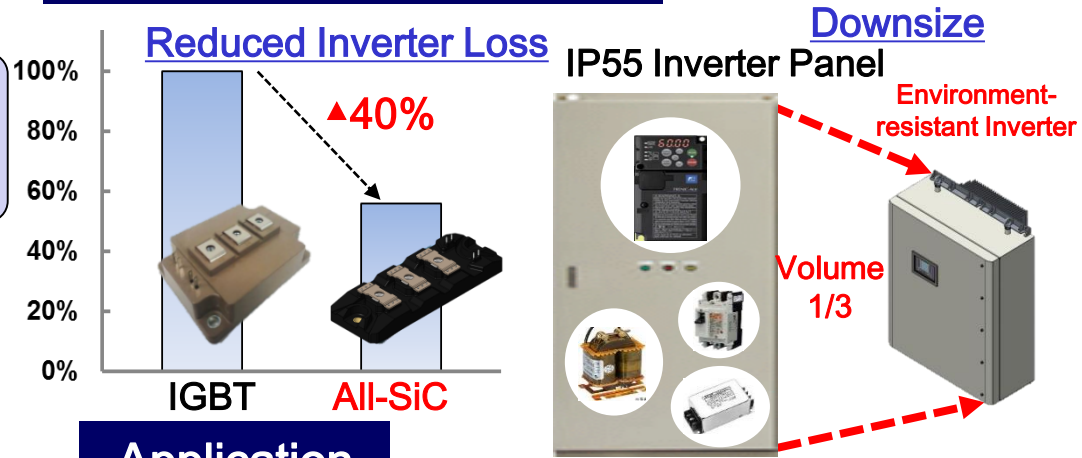
最新インバータ FRENIC-eFIT シリーズ

様々な環境にFITする強さを備えた次世代インバータ



All-SiC Module

Performance Comparison



Application

- Factory production for outdoor harsh environment

【Outdoor Pumps】



【Ventilation Fans】



【Vehicles, Tires】



Power Supply / Capacity

3 phase, 400V/3.7 ~ 37kW (Sales started)

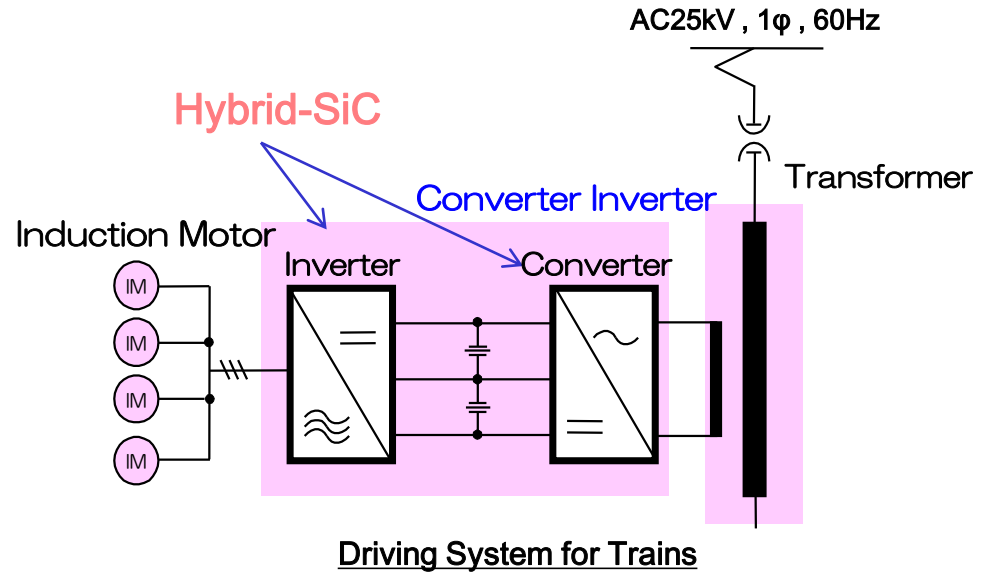
Next Gen. Shinkansen Use Hy-SiC Module **Fuji Electric** Innovating Energy Technology

- Rectifiers and inverters in N700S propulsion systems utilize Hybrid-SiC modules.
- Trial operation started in April, 2018.



Photograph by Central Japan Railway Company

N700S Test Train



3.3kV-1.8kA Rated



190×140mm
SiC-Hybrid Module



Converter Inverter

Comparison with conventional N700A

Volume : ▲10%

Weight : ▲13%

作者授权中国电源学会发布, 未经许可不得转载

New VVVF Inv. Use Hy-SiC Module

- Reduction of volume is -64%, reduction of weight is -45%.
- Commercial operation started in Oct., 2018.

New Technology

Use of SiC Devices

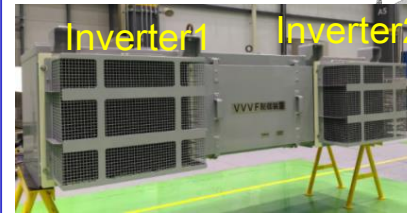
Inverter Loss:
▲20% Reduction

- Ratings : 3.3kV / 1.2kA
- Structure :
SiC Hybrid Module
IGBT(7G) + SiC-SBD

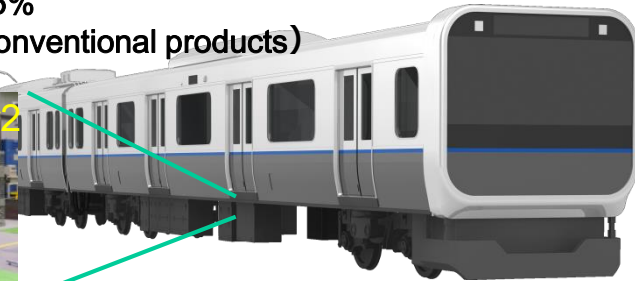


◆720kW Rated Inverter
(2-inverter unit, 4-motor drive)

- Downsize: ▲64%,
- reduction of weight: ▲45%
(comparison with Fuji conventional products)



VVVF Inverter



New Technology

Running Wind Cooling

No need for heat pipe in cooling body, simple brazing type, unit with small size and light weight

- Design based on wind-tunnel tests using fluid analysis and miniature model for train
- Confirmation of targeted performance by stationary evaluation

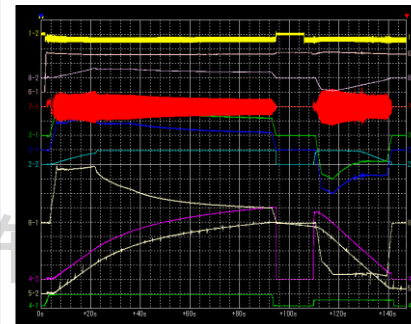


New Technology

Speed Sensorless Control

Speed Sensor is not necessary. Simplified interconnects, high reliability

- Torque error: ± 5 %
Ride quality improved



同意禁止转载

Hy-SiC Module Used in Conventional Lines **Fuji Electric** Innovating Energy Technology

□ Sanyo Electric Railway Co., Ltd. uses Hybrid-SiC Modules for its VVVF inverters.

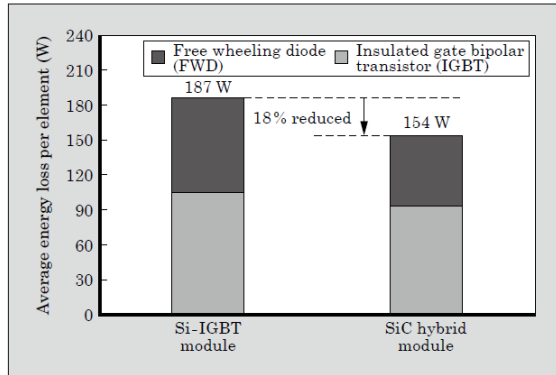


Fig.5 Energy loss comparison

1in1 1200A SiC-Hybrid Module



VVVF Inverter



山陽電鉄の5000系車両に
SiCパワー半導体を搭載した駆動用インバータ

車両の省エネルギー化とスムーズな駆動に貢献

作者授权中国电源学会发布，未经作者同意禁止转载

All-SiC Module Used in Conventional Lines

□ All-SiC modules are started to be used for VVVF in Odakyu and Marunouchi lines.

Mitsubishi module for
Odakyu line (2015/1)



小田急電鉄株式会社 1000 形車両

<https://www.zaikei.co.jp/article/20140501/191409.html>

Toshiba module for
Marunouchi line (2019/2)



<https://project.nikkeibp.co.jp/ESG/atcl/case/010900013/>

作者授权中国电源学会发布，未经作者同意禁止转载

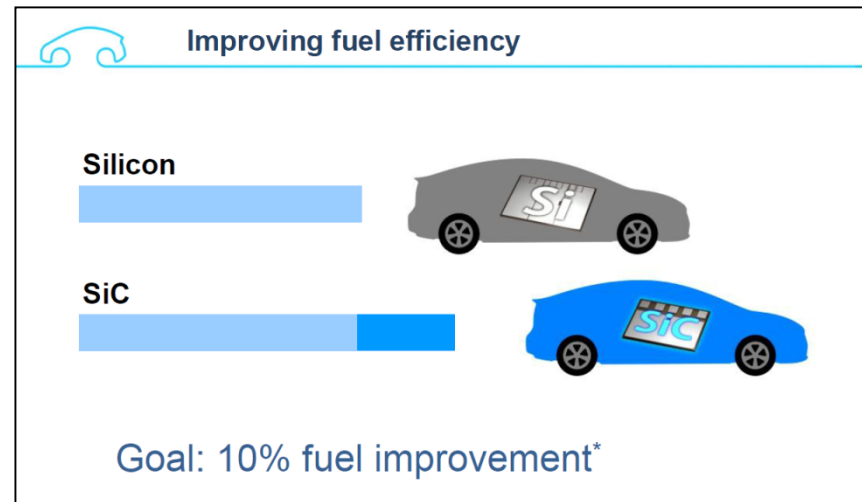
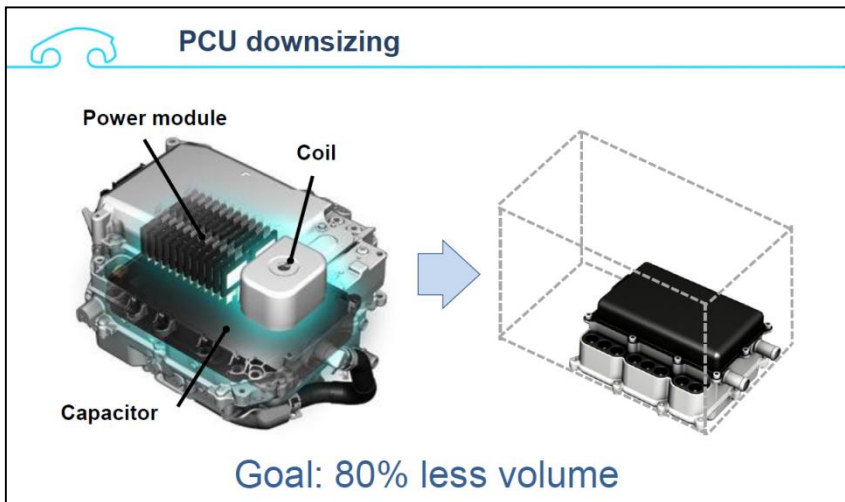
Toyota Carried out Public-Road Operation Fuji Electric Innovating Energy Technology

January, 2015 - Camry hybrid prototype with All-SiC PCU and fuel cell bus with SiC-SBD

豊田



- In the Camry hybrid prototype, Toyota is installing SiC power semiconductors (transistors and diodes) in the PCU's internal voltage step-up converter and the inverter that controls the motor.
- The bus features SiC diodes in the fuel cell voltage step-up converter, which is used to control the voltage of electricity from the fuel cell stack.



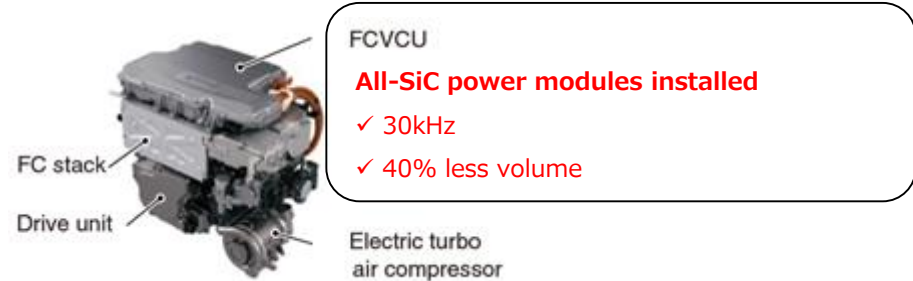
作者授权中国电源学会发布，未经作者同意禁止转载 <http://newsroom.toyota.co.jp/en/detail/5692153>
<http://newsroom.toyota.co.jp/en/detail/2656842>

Honda Started Small Number Production

March, 2016 – Clarity FC with All-SiC FC VCU released

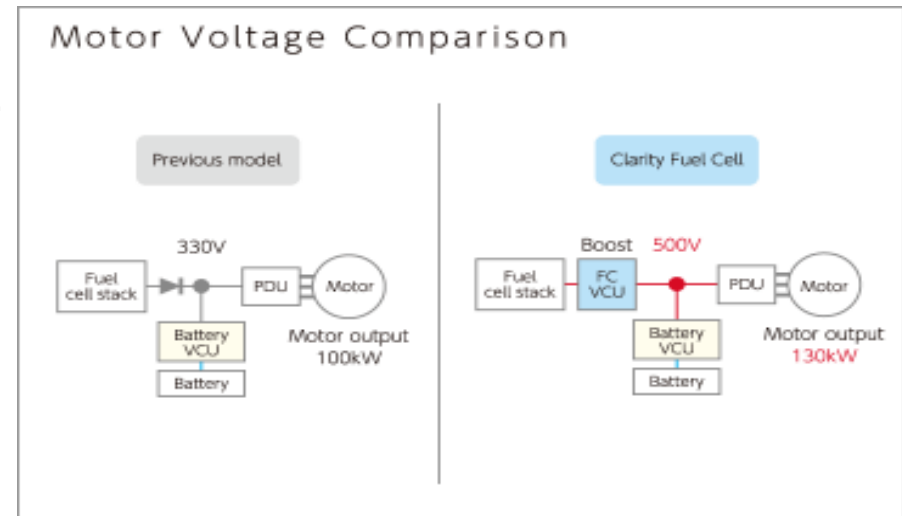
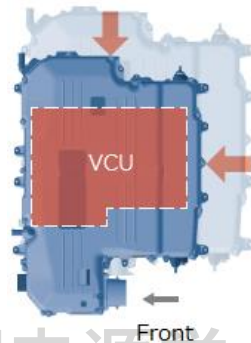
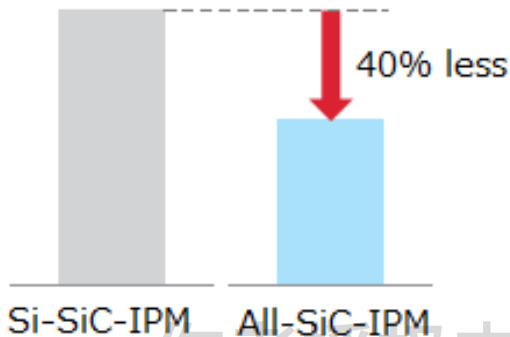
Sold 220 units by June, 2018

本田



- Sold more than 200 units by March 2018.
- Cruising range (for reference) is approximately 750 km.

Downsizing image



<http://world.honda.com/CLARITY/>

<http://world.honda.com/automobile-technology/engineer-talk/CLARITY/>

http://www.honda.co.jp/factbook/auto/CLARITY_FUEL_CELL/201603/P14.pdf

作者授权中国电源学会发布，未经许可同意禁止转载

Toyota Sells FC Bus using SiC-SBD

February, 2017 - Toyota started to sell fuel-cell bus using SiC-SBD for boost converter
 March, 2017 - Tokyo Metropolitan Bus started commercial operation of SiC FC bus and announced the plan to increase the number of SiC FC bus up to more than 100 by 2020

豊田

SiCアライアンスシンポジウム

燃料電池バス: SiCダイオード使用



出典:トヨタ自動車 ニュースリリース資料(2017年2月24日)

- ・2017年2月より、FCバスの販売を開始
- ・東京都へ2台納車、2017年3月より都営バスとして営業運行中
- ・東京オリンピック・パラリンピックに向けて100台以上の導入予定

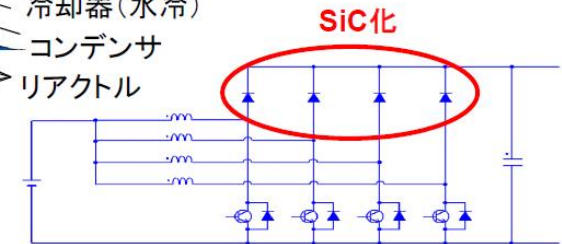
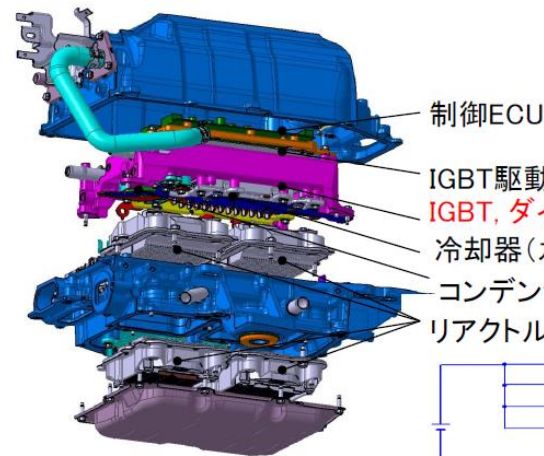
SiCアライアンスシンポジウム

FC昇圧コンバータ概要

41

主要特性

最高電圧	650 V
容量	13 L
相	4相
冷却方法	水冷



4相昇圧コンバータ回路図

FCバスでは、昇圧コンバータにSiCダイオードを採用

Keikyu Started FC Bus using SiC-SBD

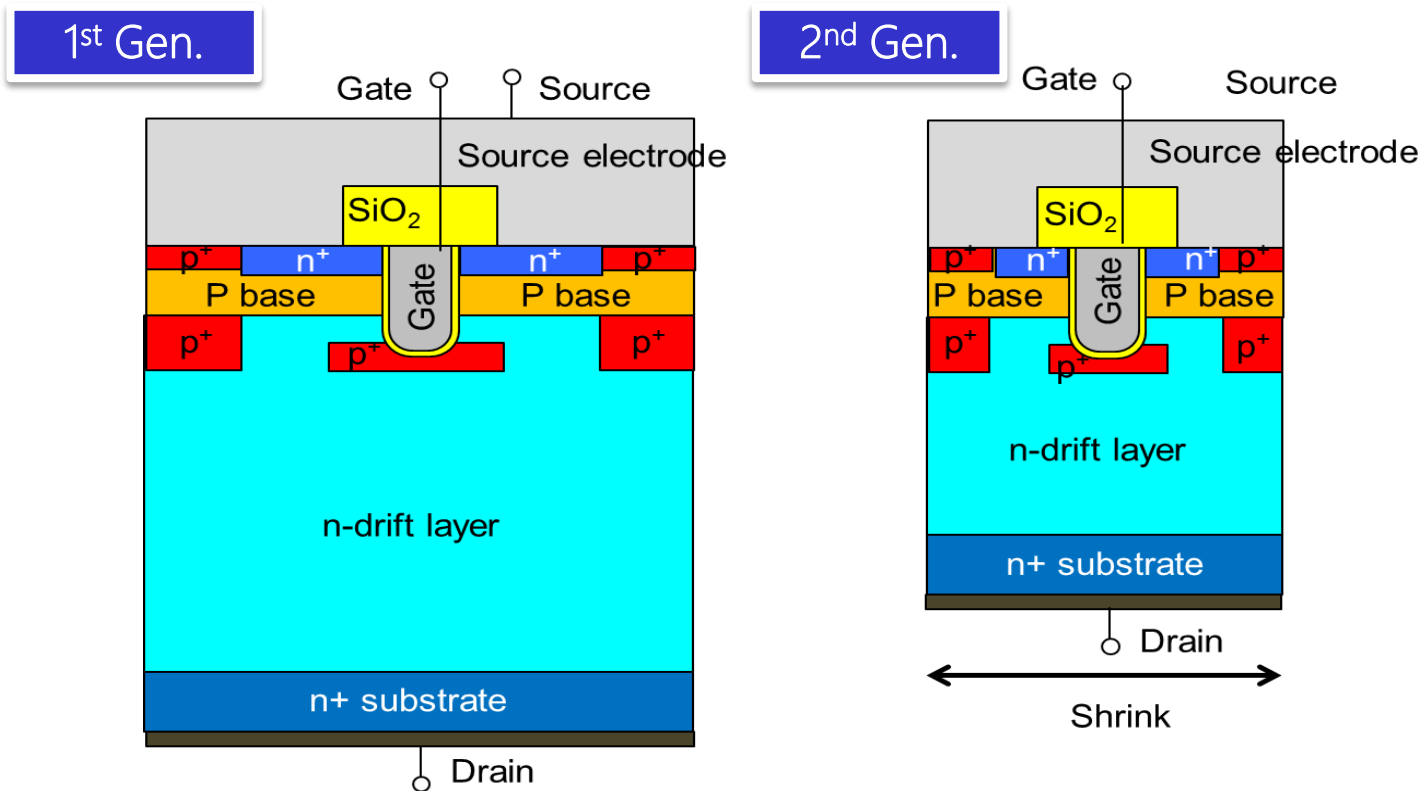
February, 2019 – Keikyu Bus started operation of FC bus “SORA” using SiC-SBD in Odaiba area.



作者授权中国电源学会发布，未经作者同意禁止转载

<https://response.jp/article/2019/02/25/319479.html>

Cross-Section Structure of SiC MOSFETs

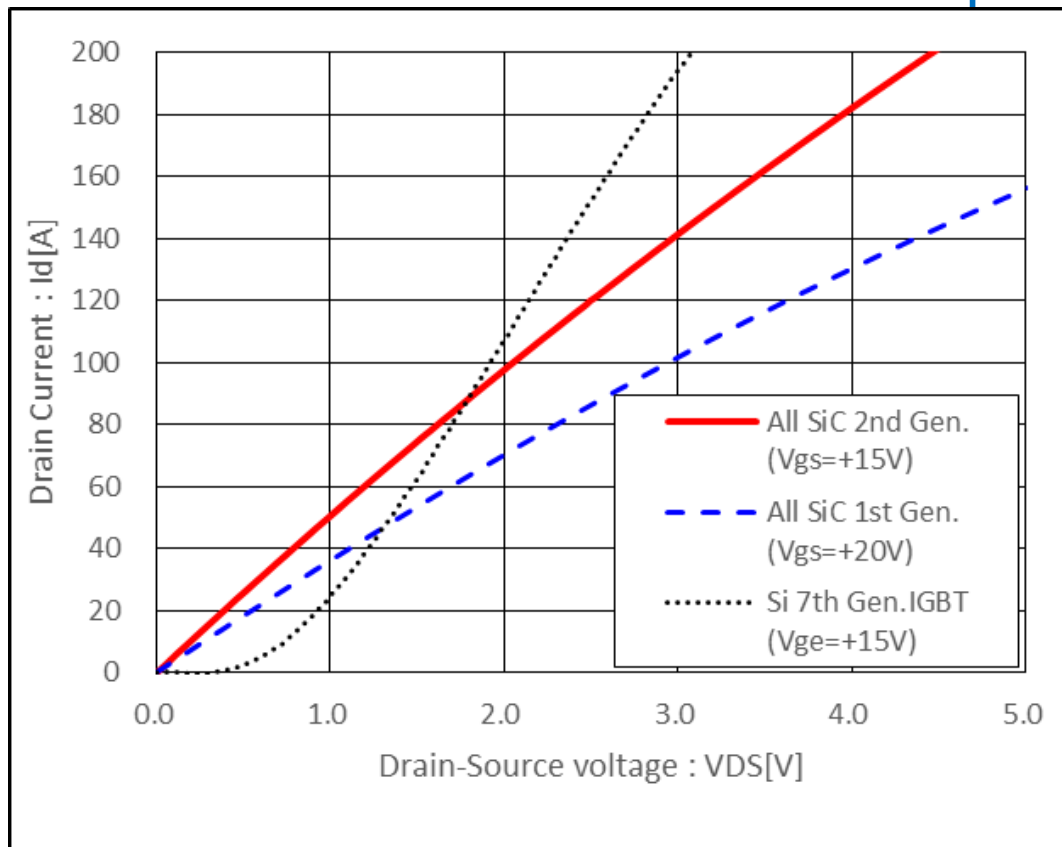


comparison of characteristics (1200V)

	1 st Gen. trench gate SiC MOSFETs	2 nd Gen. trench gate SiC MOSFETs
Normalized RonA	1.00	0.77
V _{GS(th)}	5.1V	5.0V
Recommended Gate Voltage	+20/-3V	+15/-3V

Si 7th Gen./All-SiC1st Gen./All-SiC2nd Gen. output characteristic

1200V/100A



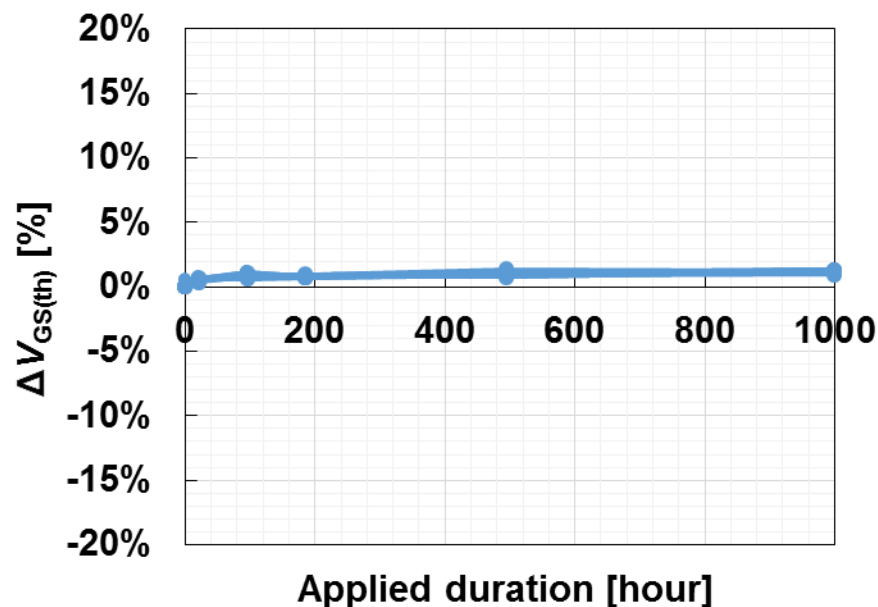
All-SiC output characteristic was improved!

→ The on-state voltage of all-SiC module was reduced under 85A.

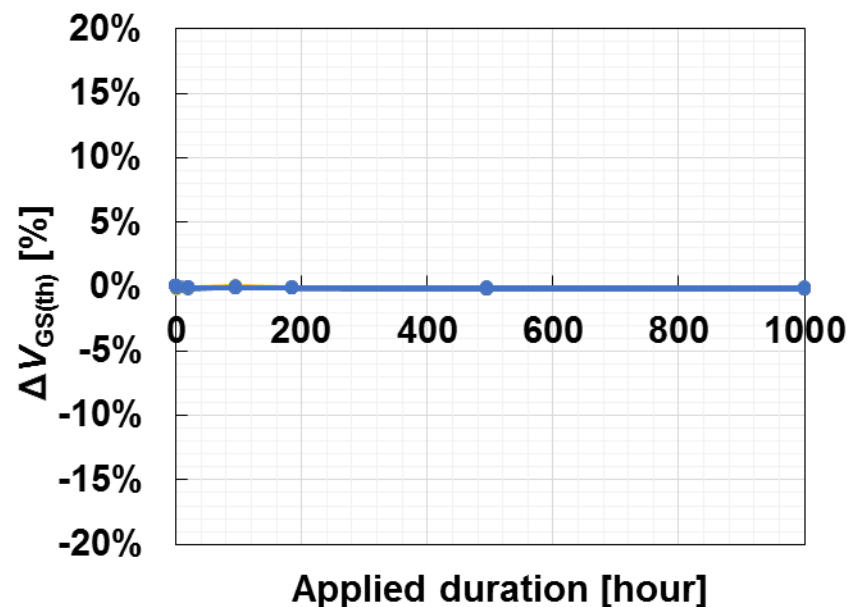
作者授权中国电源学会发布，未经作者同意禁止转载

Reliability test results under DC biased condition to All-SiC 2nd Gen.

(a) $T_{vj}=175\text{deg.C}$ $V_{gs}=+20\text{V}$



(b) $T_{vj}=175\text{deg.C}$ $V_{gs}=-7\text{V}$



Gate characteristics of 2nd generation trench gate SiC MOSFETs is stable.
→ Realize high reliability for All-SiC modules.

作者授权中国电源学会发布，未经作者同意禁止转载

All-SiC lineup plan

		Package Type	Small 1B	Small 2B	62mm STD	HPnC
		Size (WxDxH)	62.8x33.8x12 mm	56.7x62.8x12 mm	62x108x30.5 mm	100x140x38 mm
Rated voltage	MOSFET generation	Equivarent Circuit				
1200V	2 nd generation Trench gate	2in1	~100A	~200A	~600A	N/A
		6in1	~50A	~100A	N/A	N/A
1700V	2 nd generation Trench gate	2in1	N/A	N/A	~400A	TBD
3300V	1 st generation Trench gate	2in1	N/A	N/A	N/A	~750A

The product lineup will realize coverage of the wide range inverter capacity.

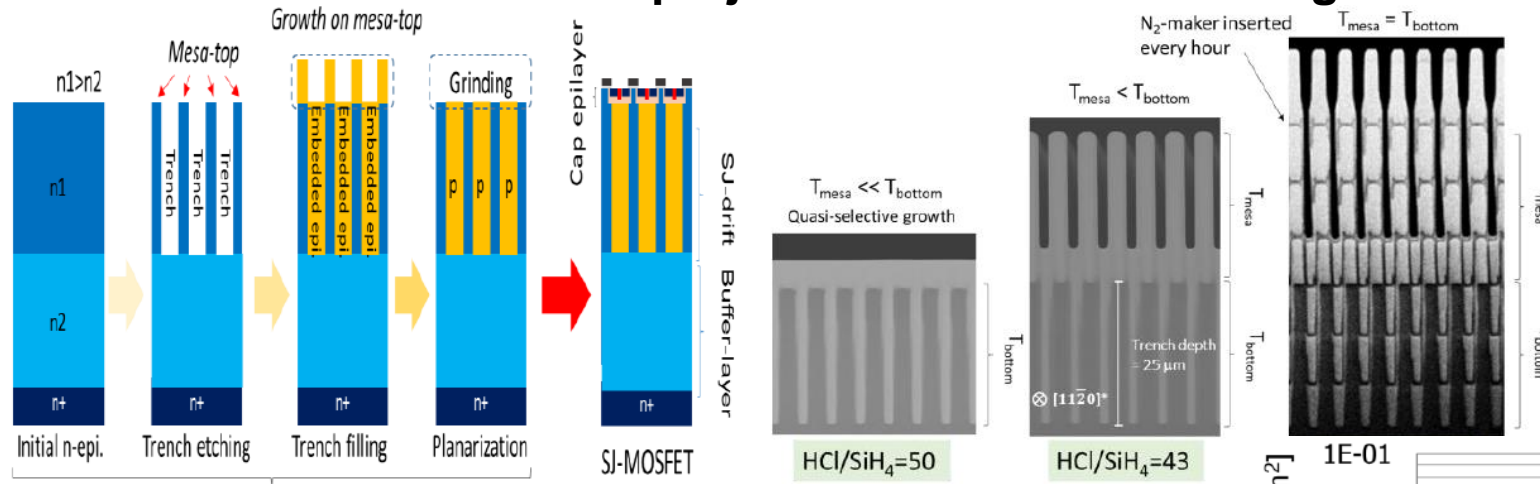
作者授权中国电源学会发布，未经作者同意禁止转载

□ Advanced SiC Devices

作者授权中国电源学会发布，未经作者同意禁止转载

6.5kV SiC Superjunction MOSFET

□ 7.8kV 17.8mΩcm² SiC Superjunction MOSFET breaking the 4H-SiC unipolar limit.



SJ wafer fabrication process integrating four element technologies

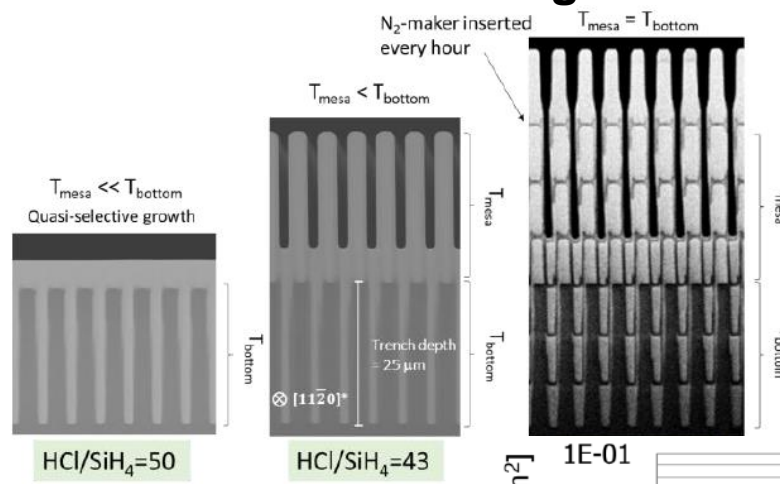


Figure 2. Cross-sectional SEM images of SJ-MOSFETs under different TFE growth conditions in terms of

Figure 1. Schematic of a fabrication process of partial SJ structure by trench-filling epitaxial (TFE) growth method. The partial-SJ structure consists of the SJ-drift part and n-type buffer layer (n₁>n₂).

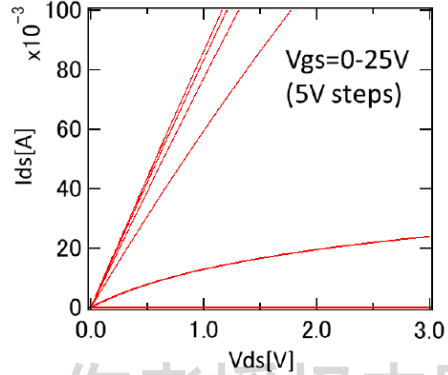


Figure 8. Ids-Vds of SJ MOSFET at RT.

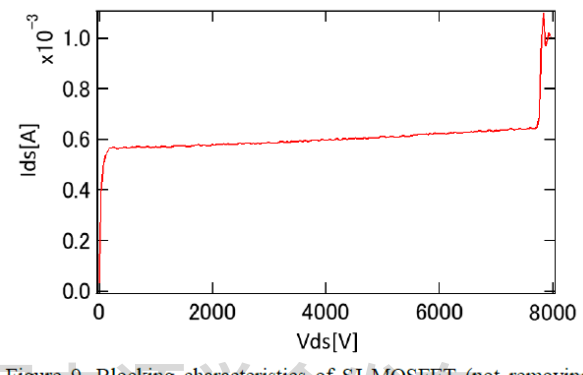


Figure 9. Blocking characteristics of SJ MOSFET (not removing voids by cleavage).

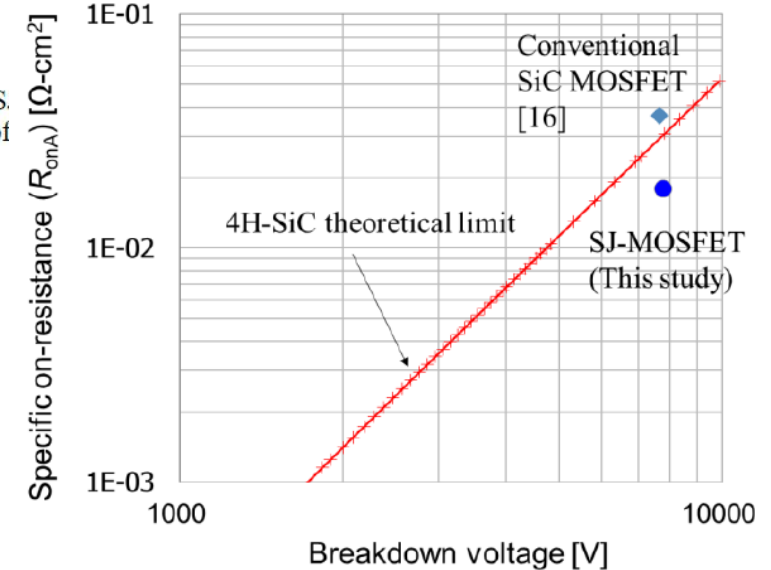


Figure 10. Trade-off relationship between specific resistivity of drift layer and breakdown voltage. Blue circle corresponds to this study.

1.2kV SiC SuperjunctionTrench MOSFET

Dynamic operations of rugged SiC Superjunction MOSFET with $BV_{dss}=1.6kV$.

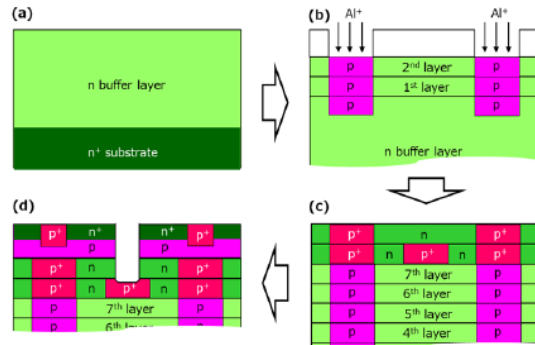


Fig. 4. Fabrication flow of SiC SJ-UMOSFET through multi-epitaxial growth method.

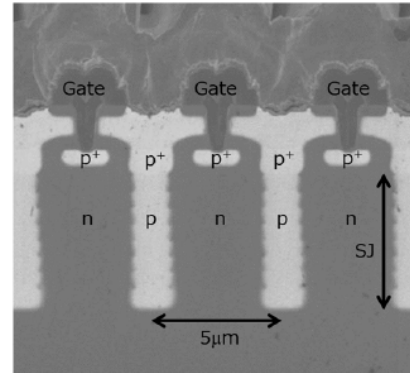


Fig. 5. SEM image of developed 1.2-kV class SiC SJ-UMOSFET.

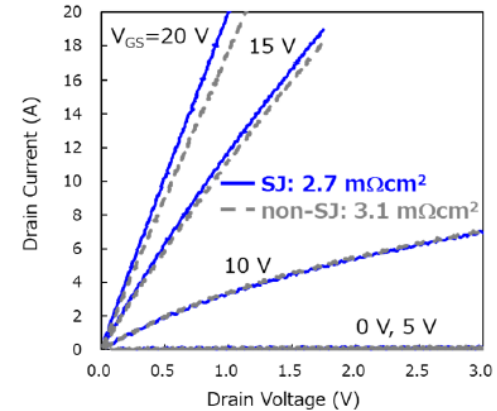


Fig. 6. Typical output characteristics of SJ- and non-SJ-UMOSFET. The R_{onA} was measured at a drain current of 18 A and a gate voltage of 20 V.

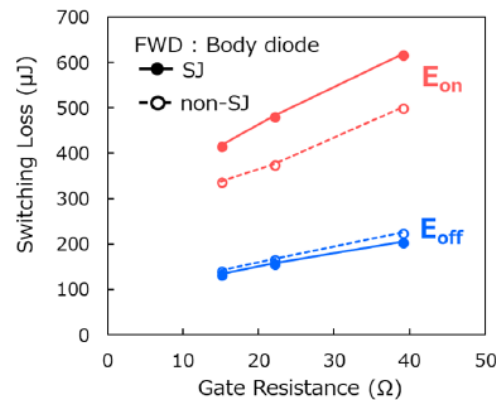


Fig. 16. Gate resistance dependences of switching energies for turn-on and turn-off of SJ- and non-SJ-UMOSFET with internal body diode as freewheeling diode.

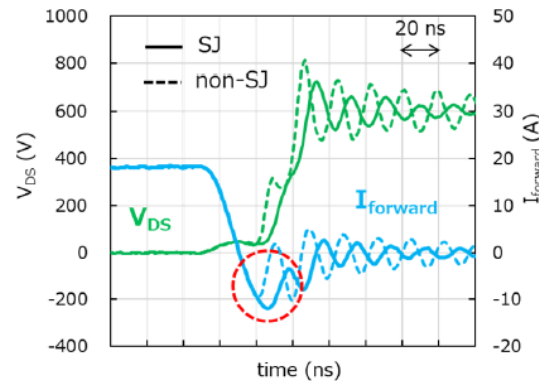


Fig. 17. Reverse recovery waveform of the body diode as freewheeling diode in SJ- and non-SJ-UMOSFET.

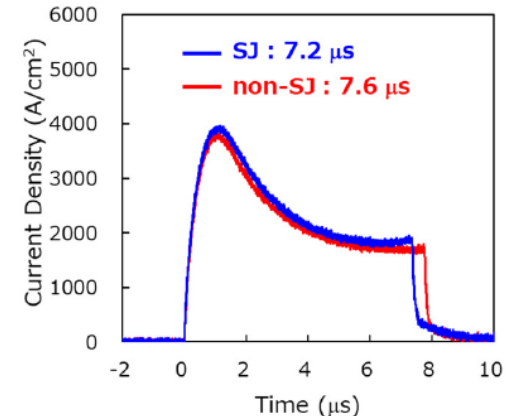


Fig. 18. Short circuit waveforms of SJ- and non-SJ-UMOSFET.

作者授权中国电源学会发布，未经作者同意禁止转载

1.2kV SiC Superjunction Trench MOSFET

- Dramatic reduction of on-resistance at elevated temperature and low-loss and rugged reverse recovery of SiC Superjunction MOSFET with $BV_{dss}=1.6kV$.

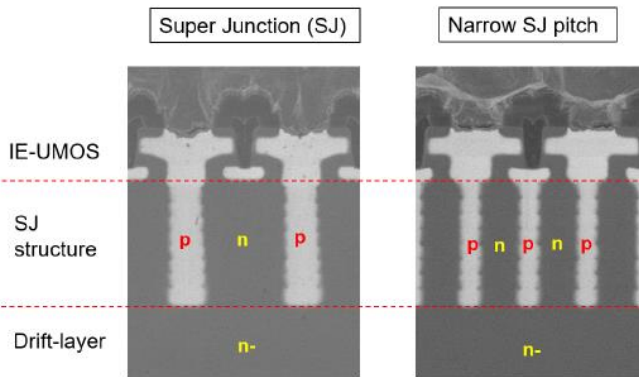


Fig. 2 SEM micrographs of fabricated SJ MOSFETs

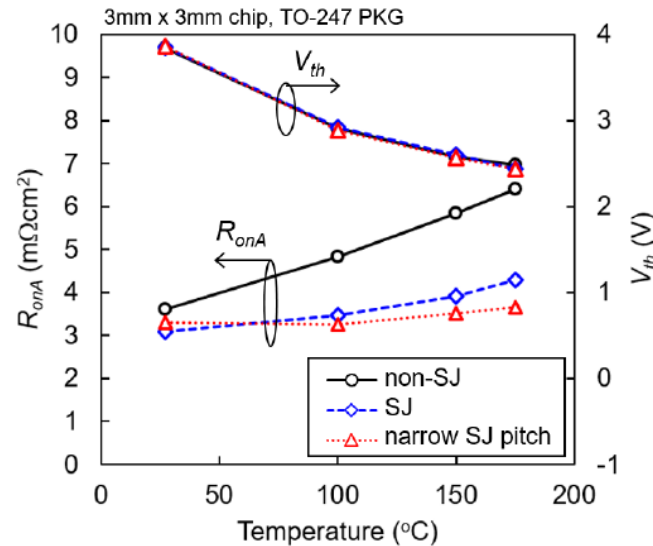


Fig. 4 Temperature dependency of R_{onA} and V_{th}

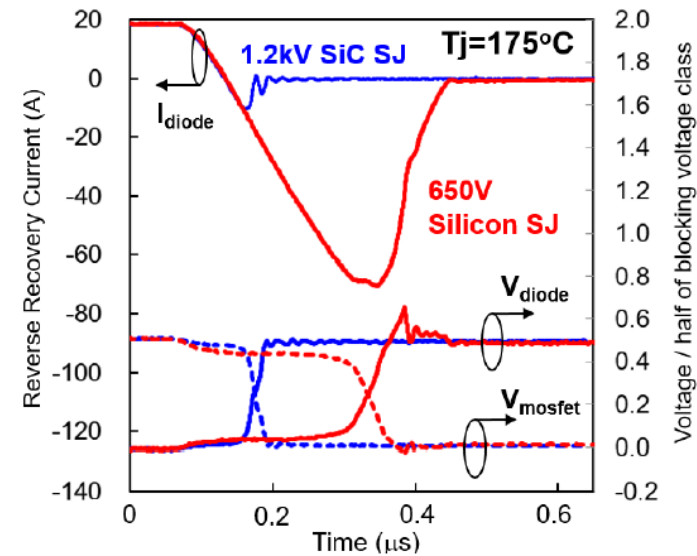


Fig. 15 Reverse recovery of the Si and SiC SJ devices

作者授权中国电源学会发布，未经作者同意禁止转载

0.63mΩcm² SiC Superjunction MOSFET

□ Extremely low specific on-resistance 0.63mΩcm²/1170V close to SiC unipolar limit.

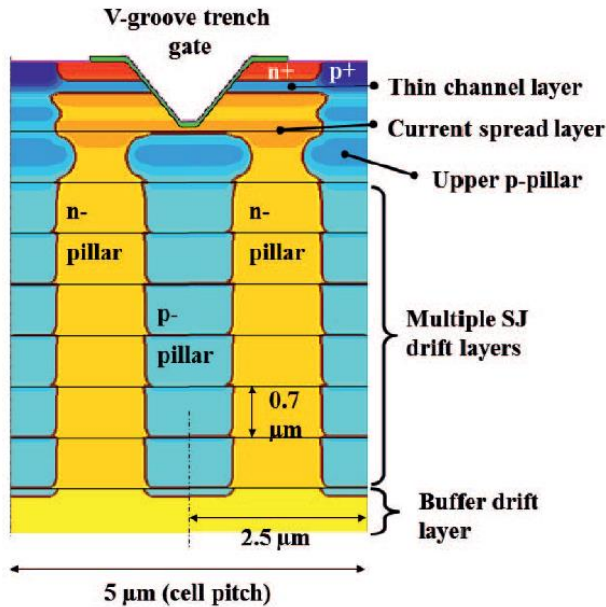


Fig. 1. A schematic cross section of the SJ-VMOSFET.

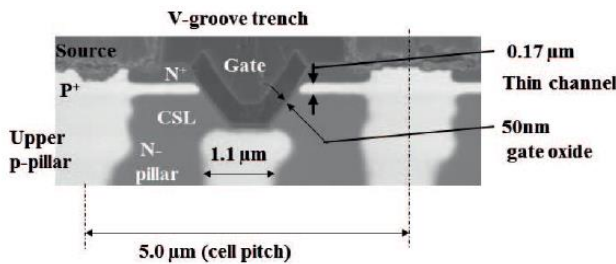


Fig. 2. An SEM image of the fabricated SJ-VMOSFET with the ultra-thin channels.

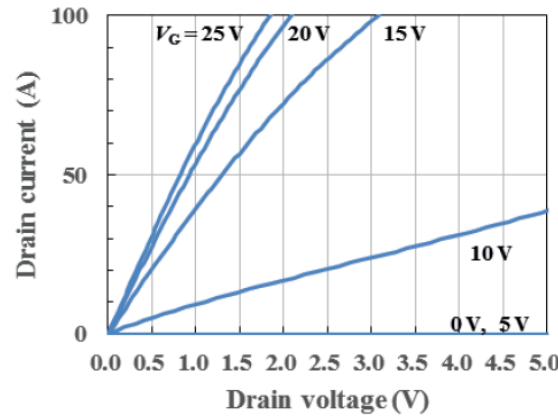


Fig. 4. Output characteristics of the SJ-VMOSFET with the active area of 0.0377cm².

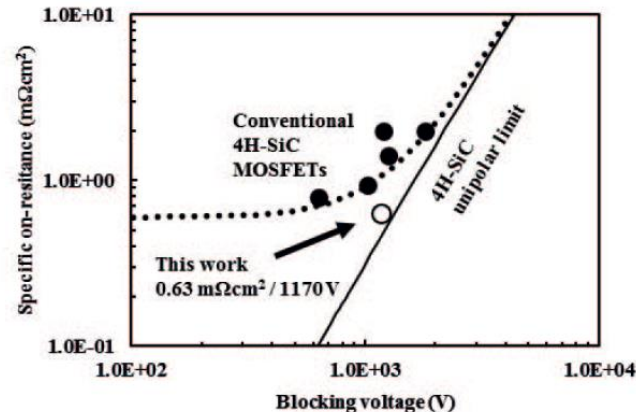


Fig. 8. Tradeoff relationship between $R_{on,sp}$ and B_V of 4H-SiC MOSFETs.

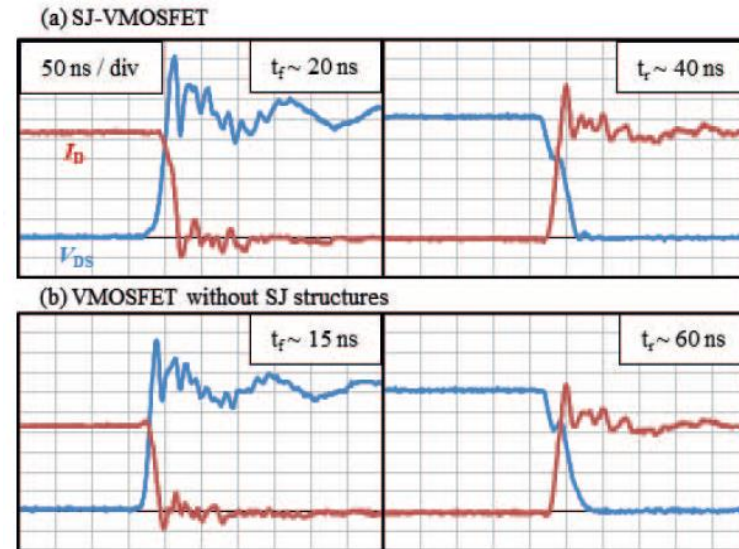


Fig. 11. Switching waveform comparison between the SJ-VMOSFET (a) and the VMOSFET without SJ structures (b).

Latest Situation of SiC IGBT, Dec. 2018

6kV 60A switching up to 250°C by 8.0mmx8.0mm 16.5kV SiC IGBT.

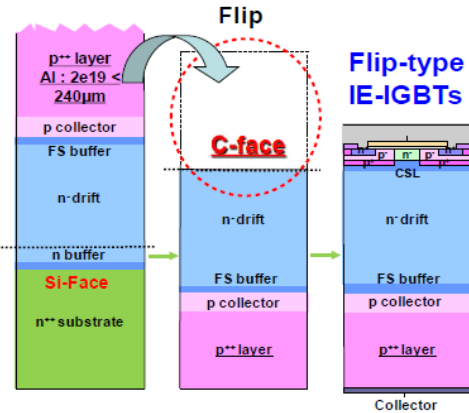


Fig. 11. Process flow of Flip-type IE-IGBT.

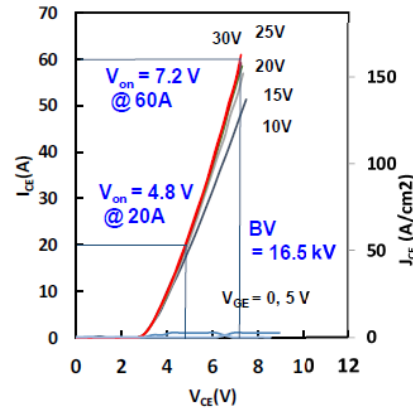


Fig. 12. On state characteristics of the 8 mm × 8 mm 16 kV IE-IGBT.

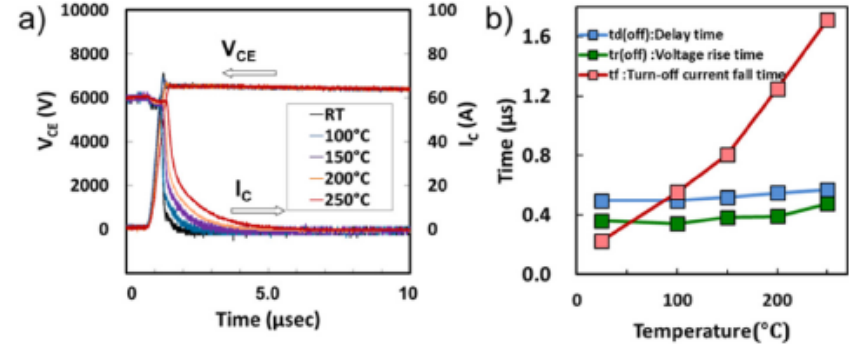


Fig. 13. a) Turn-off switching waveforms and b) Turn-off current fall time of the 8 mm × 8 mm IE-IGBTs.

10kV 100A switching up to 200°C by 4X 5.3mmx5.3mm 16.5kV SiC IGBT.

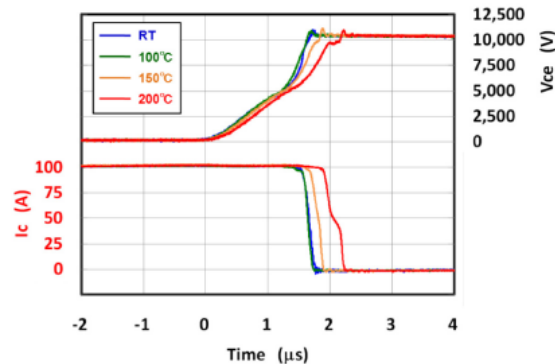


Fig. 14. Demonstration of 1 MVA turn-off switching wave form of four IGBTs parallel in one module.

New project: 20kV-class SiC IGBT under development.

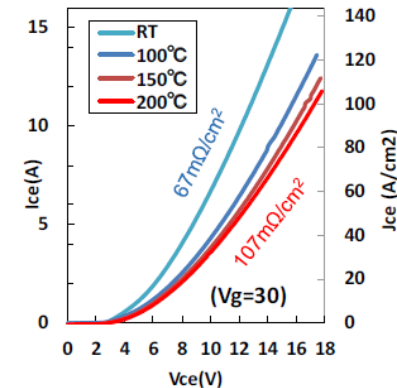


Fig. 15. On-state characteristics of the 20-kV class IE-IGBTs.

作者授权中国电源学会发布 未经作者同意禁止转载

Latest Situation of SiC IGBT, Sep. 2019

□ 26.8kV, 36.9mΩcm²@100A/cm², V_{ce(sat)}=8.2V@100A/cm², SiC IGBT demonstrated.

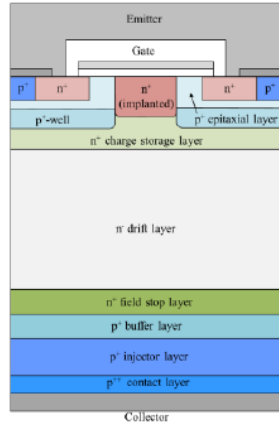


Fig. 1. Schematic cross-section of n-IE-IGBTs.

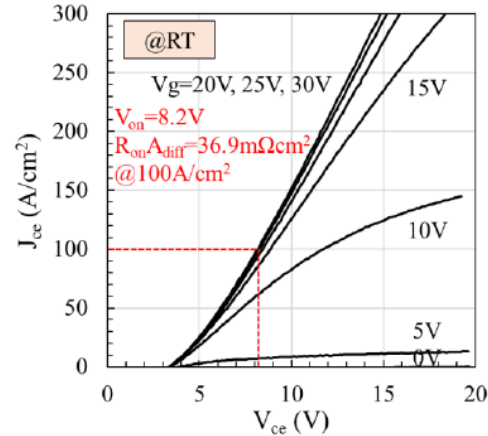


Fig. 2. On-state I-V characteristics of the n-IE-IGBT at room temperature.

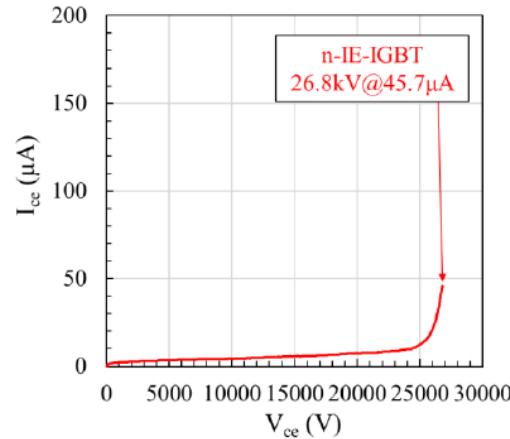


Fig. 3. Blocking characteristics of the n-IE-IGBT.

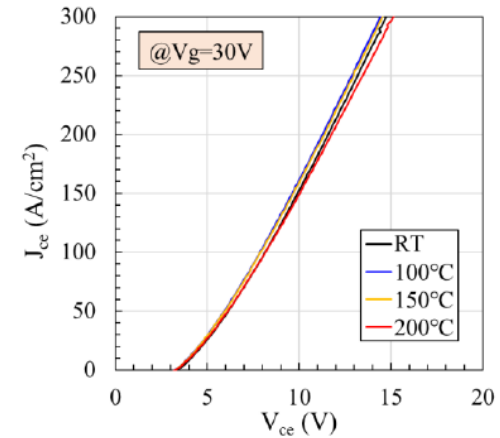


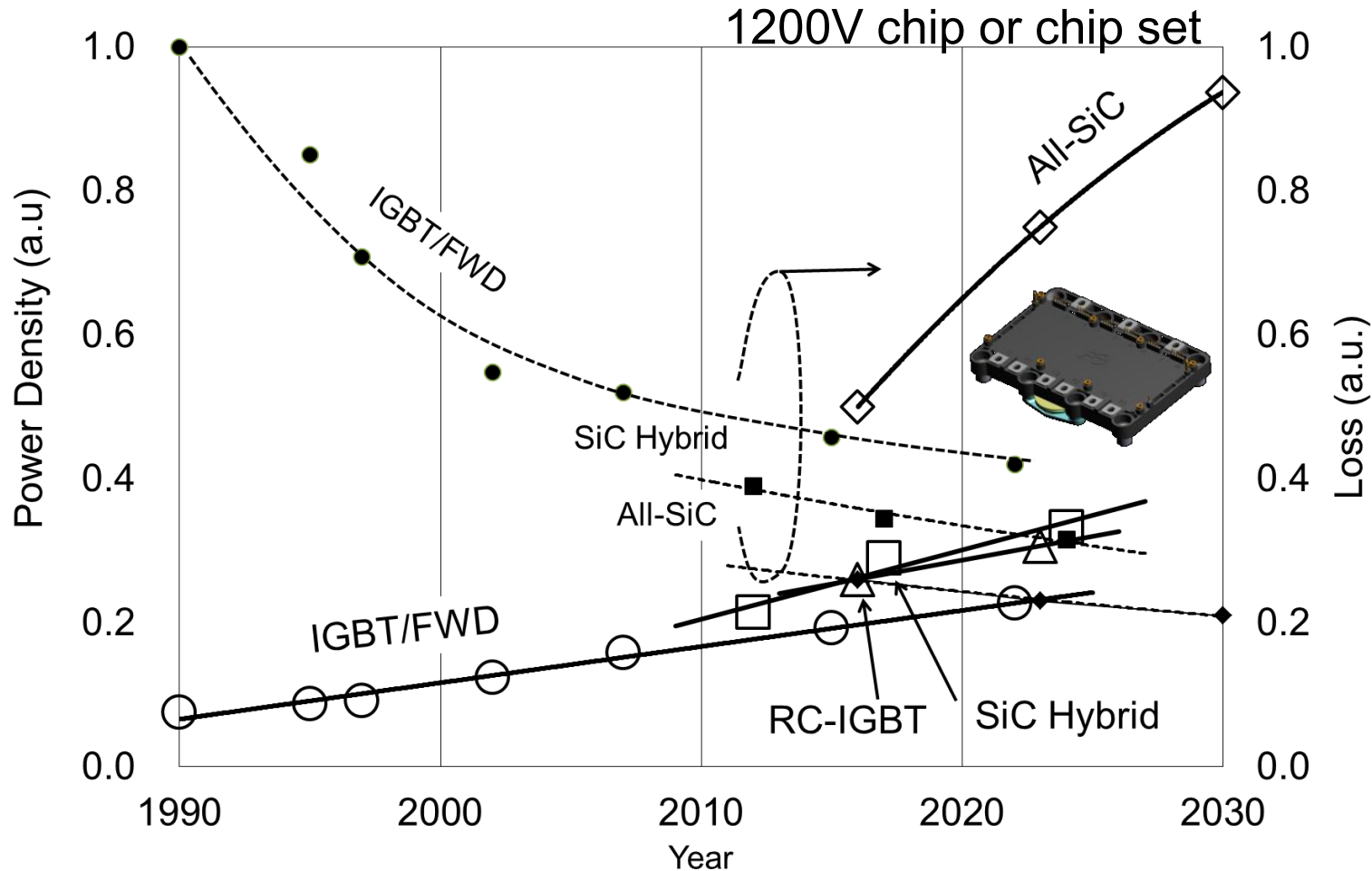
Fig. 4. Temperature dependence of on-state I-V characteristics of the n-IE-IGBT at the gate voltage of 30V.

作者授权中国电源学会发布 未经作者同意禁止转载

□ Conclusions

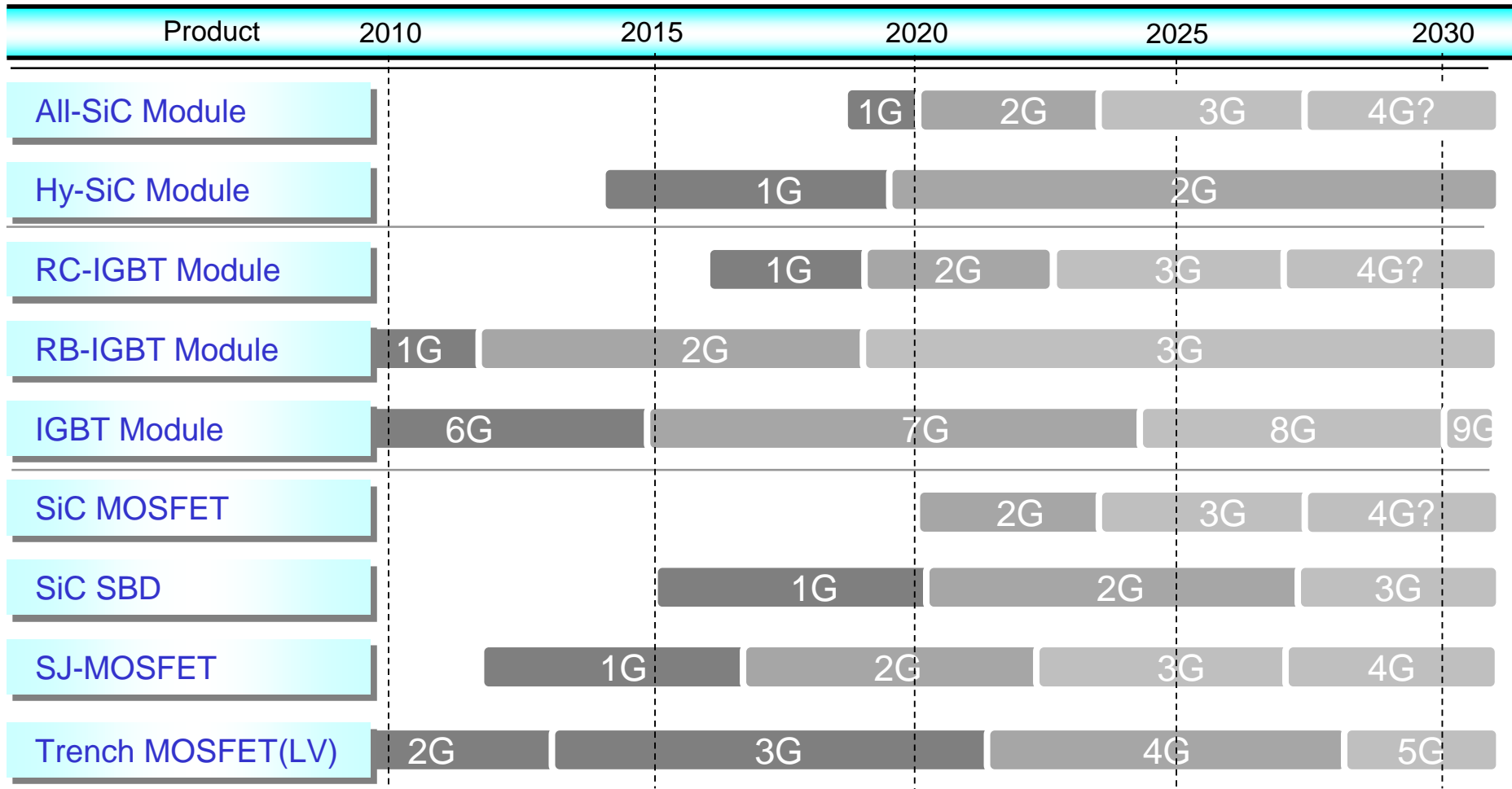
作者授权中国电源学会发布，未经作者同意禁止转载

Trend and Forecast of Power Density and Loss of Power Device Chips



Power Density: Power Rating (Voltage x Current) / Total Chip Area
Loss: Estimated Total Power Dissipation in 400VAC General Purpose Inverter

Fuji's Roadmap of Power Semiconductor Devices



Indication by chip generation

作者授权中国电源学会发布，未经作者同意禁止转载

Thank you!

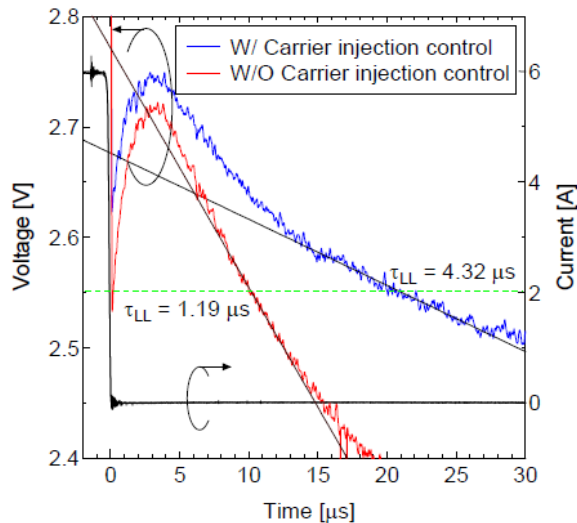
FE Fuji Electric
Innovating Energy Technology

Acknowledgment

Some part of this work has been implemented under a joint research project of Tsukuba Power Electronics Constellations (TPEC).

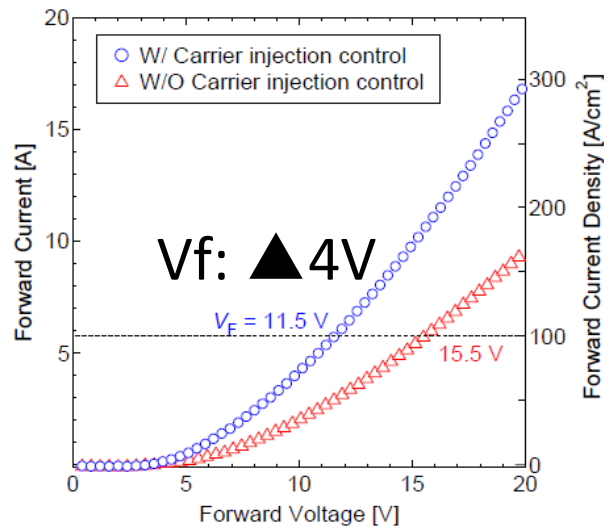
27.5kV PiN Diode with Low Vf

- The low-level carrier lifetimes (t_{LL}) of the PiN diodes were calculated from the OCVD waveform slopes at 2.55 V, being **4.32 and 1.19 μ s** for the diodes fabricated with and without carrier injection control, respectively
- By introducing carrier injection control, the **Vf of fabricated PiN diode decreased from 15.5 to 11.5 V**.
- The VB of the fabricated PiN diode was 27.5 kV, which is the highest yet reported for 20-A 4H-SiC PiN diode.

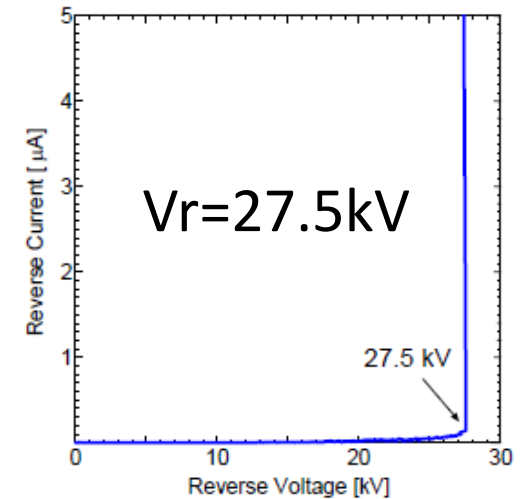


OCVD waveforms of fabricated PIN diodes

OCVD:Open Circuit Voltage Decay



Forward Characteristics of Fabricated PiN Diodes



Reverse Characteristics of Fabricated PiN Diode

SBD-Integrated SiC Trench MOSFET

Body PiN diode inactivation with low on-resistance achieved by a 1.2 kV-class 4H-SiC SWITCH-MOS

Yusuke Kobayashi^{1,2}, Naoyuki Ohse¹, Tadao Morimoto², Makoto Kato², Takahito Kojima¹, Masaki Miyazato^{1,2},
Manabu Takei^{1,2}, Hiroshi Kimura¹ and Shinsuke Harada²

¹Fuji Electric Co., Ltd., Matsumoto, Nagano, Japan, email: yusuke-kobayashi@aist.go.jp, kobayashi-yusuk@fujielectric.com

²National Institute of Advanced Industrial Science and Technology (AIST), Tsukuba, Ibaraki, Japan

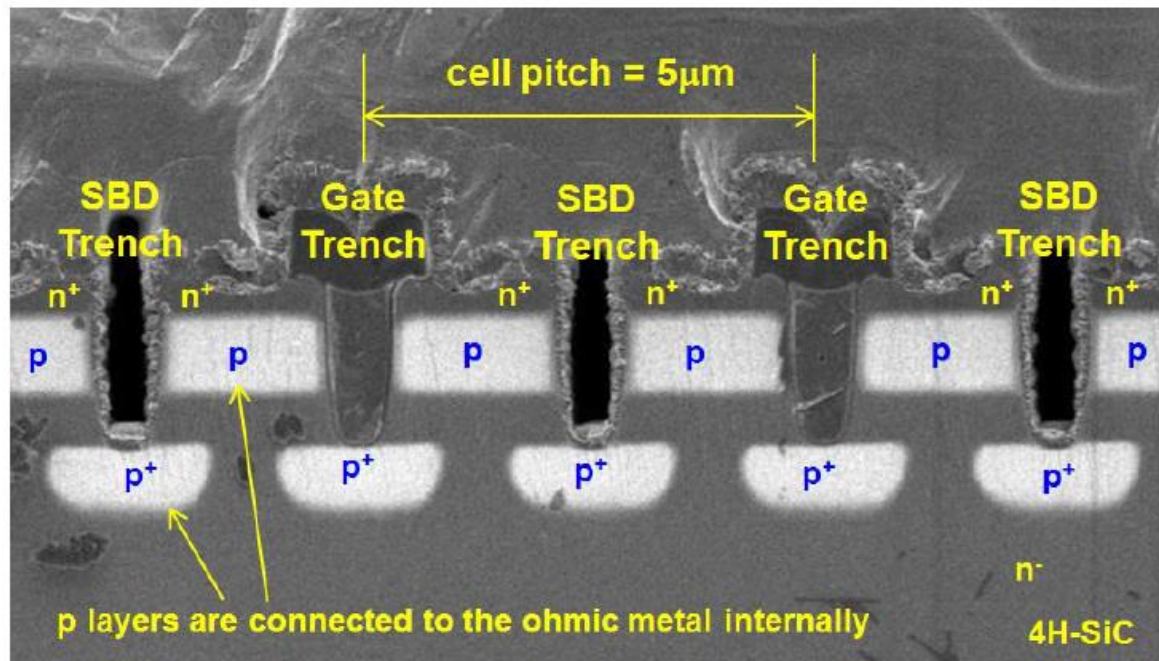


Fig. 8. Cross-sectional SEM image of the SWITCH-MOS with a 5 μm cell pitch

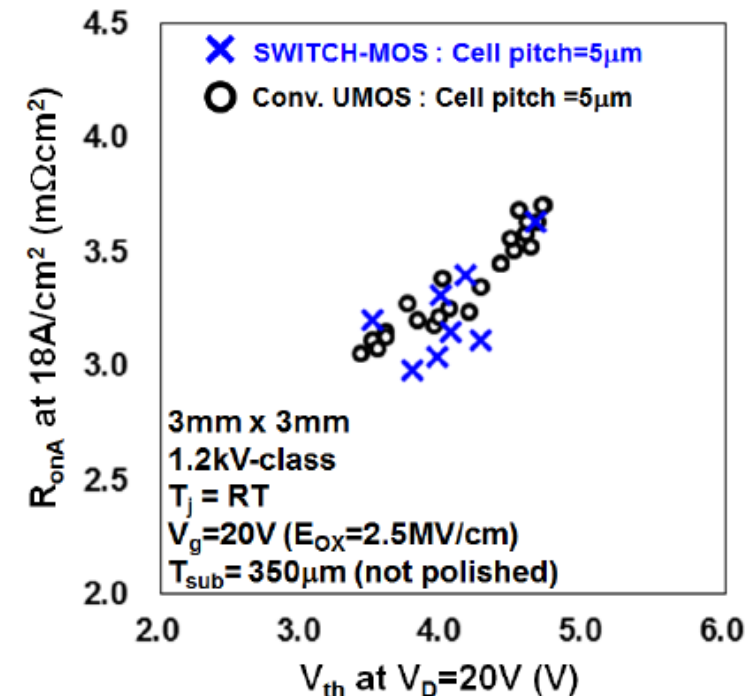


Fig. 10. R_{onA} - V_{th} trade-off in the SWITCH-MOS and conventional UMOS

SBD-Integrated SiC Trench MOSFET

➤ No degradation of Ron or Vf up to 1500A/cm² reverse current conduction

1200V Device

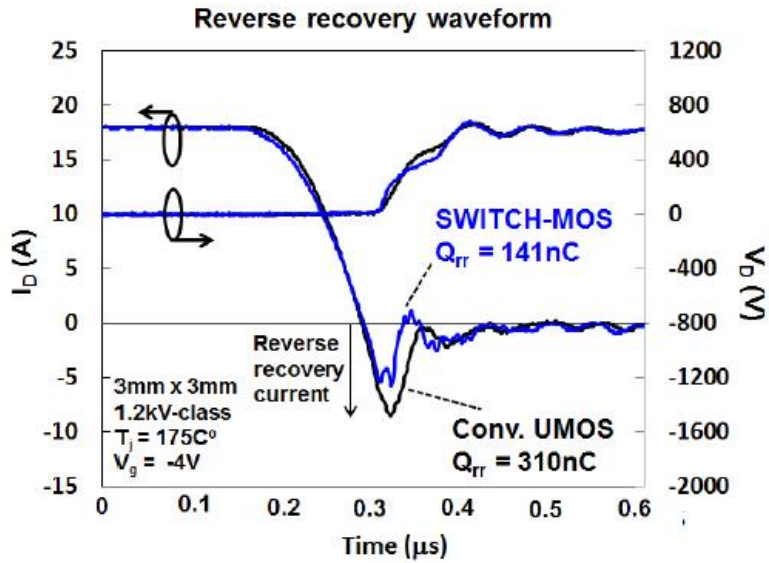


Fig. 13. Reverse recovery waveform of the body diode as a freewheeling diode in the SWITCH-MOS and conventional UMOS

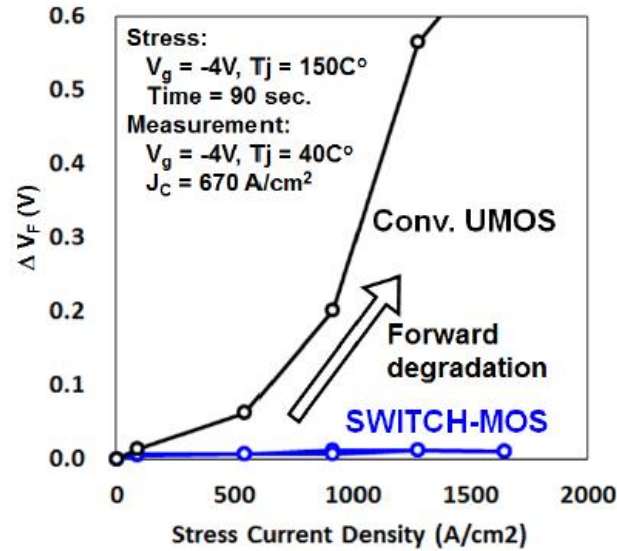


Fig. 14. Forward degradation as a function of forward current stress in the SWITCH-MOS and conventional UMOS

SWITCH-MOS
Cell Pitch = $5\mu\text{m}$

no visible
stacking faults



Conv. UMOS
Cell Pitch = $5\mu\text{m}$

expanded
stacking faults
with white bands
and triangles



Fig. 15. Photoluminescence mapping images of stacking faults after stress of $1640 \text{ A}/\text{cm}^2$ for 90 seconds

- The **halo implanted** high acceptor concentration region behind the channel blocks the penetration of the depletion region into the p-base. Since the short channel effect is suppressed without increasing the acceptor concentration in the channel, high channel mobility is maintained by low acceptor concentration.
- **Low RonA of 2.0 mΩcm² with high Vth of 4V achieved on the 1.2kV MOSFET.**

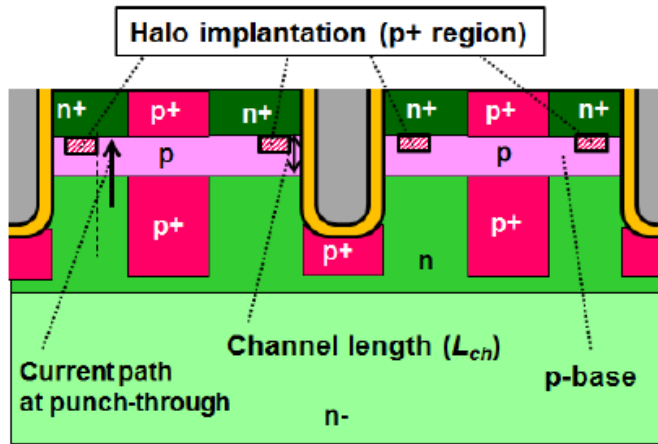


Fig. 1. Schematic cross-section of the halo implanted 4H-SiC IE-UMOS

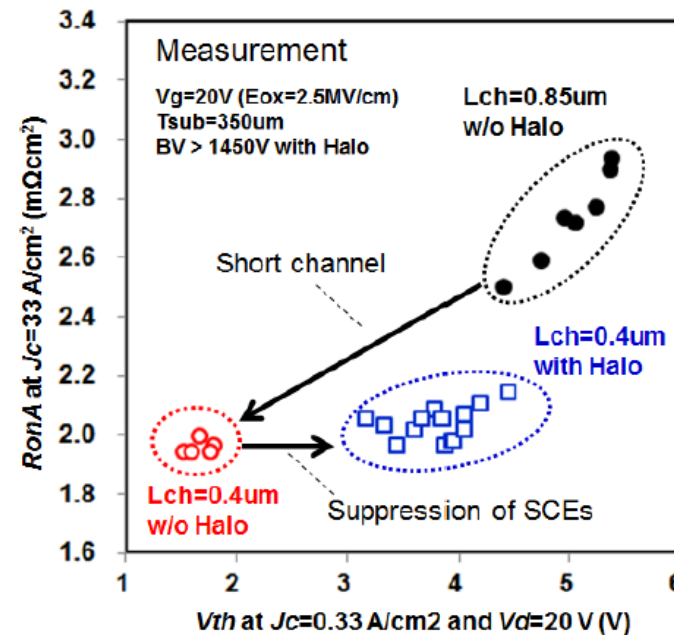
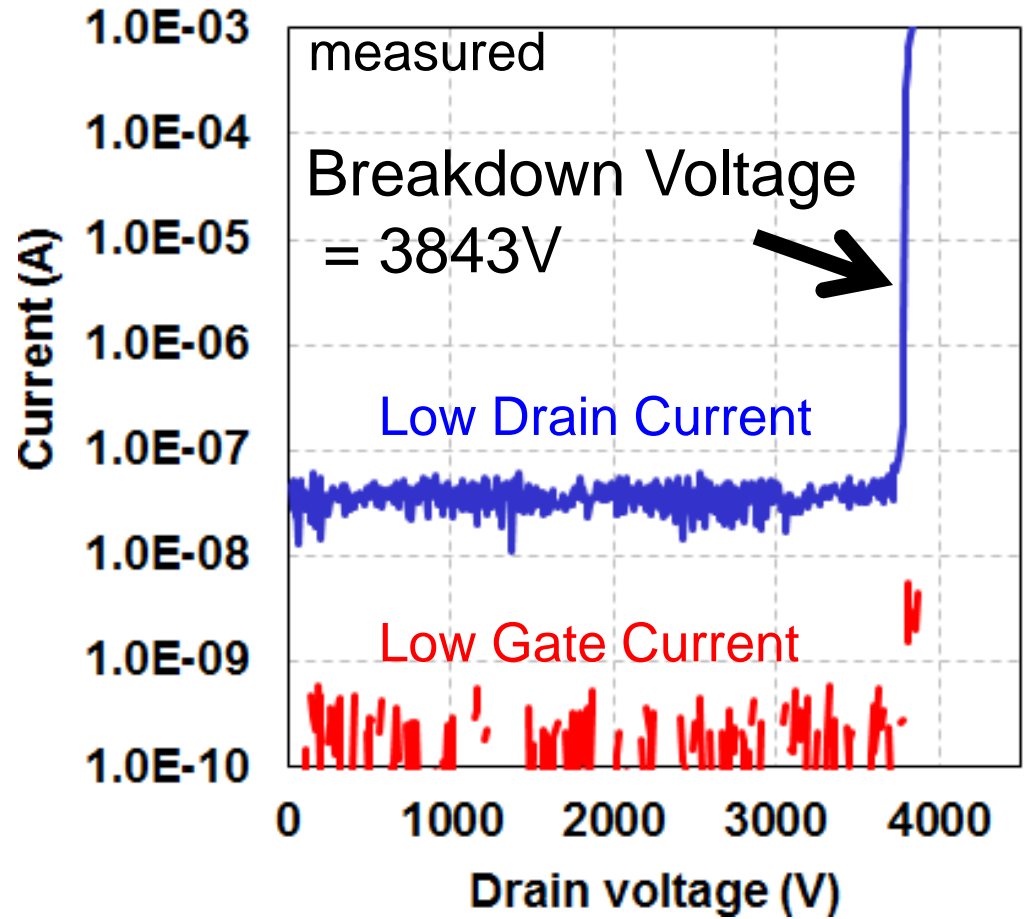
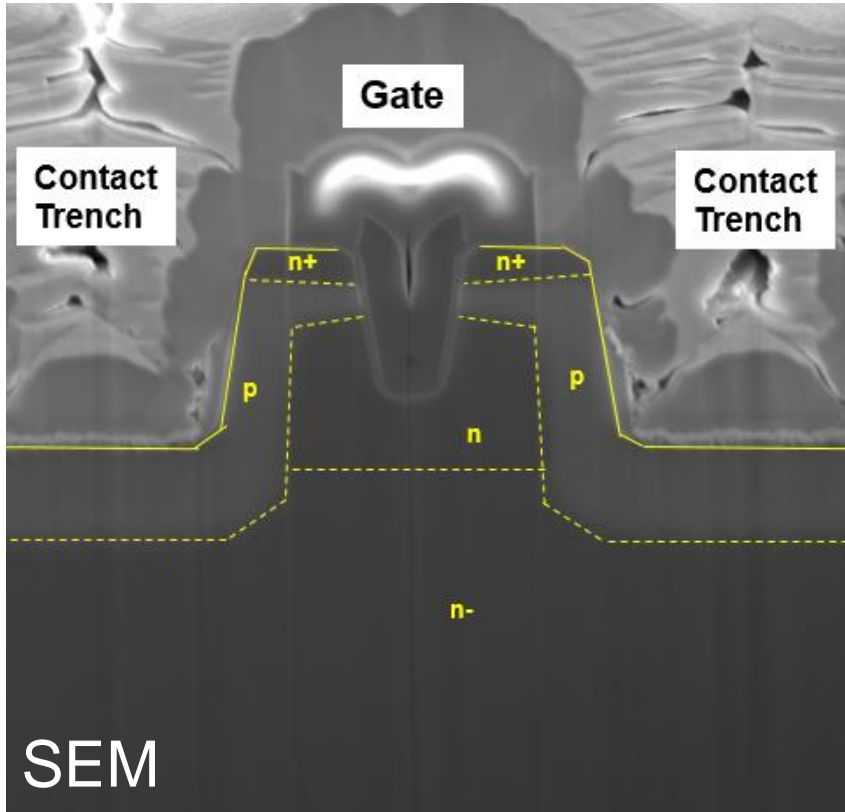


Fig. 4. Trade-off between R_{onA} and V_{th} in the fabricated IE-UMOS, with and without halo implantation.

3.3kV SiC Trench MOSFET



Break down voltage of 3843V was achieved with small gate current

作者授权中国电源学会发布, 未经作者同意禁止转载

[Ref.] Y. Kobayashi, et. al., ICSCRM, 2015

□ Comparison of Si, Hybrid-SiC, and All-SiC Modules

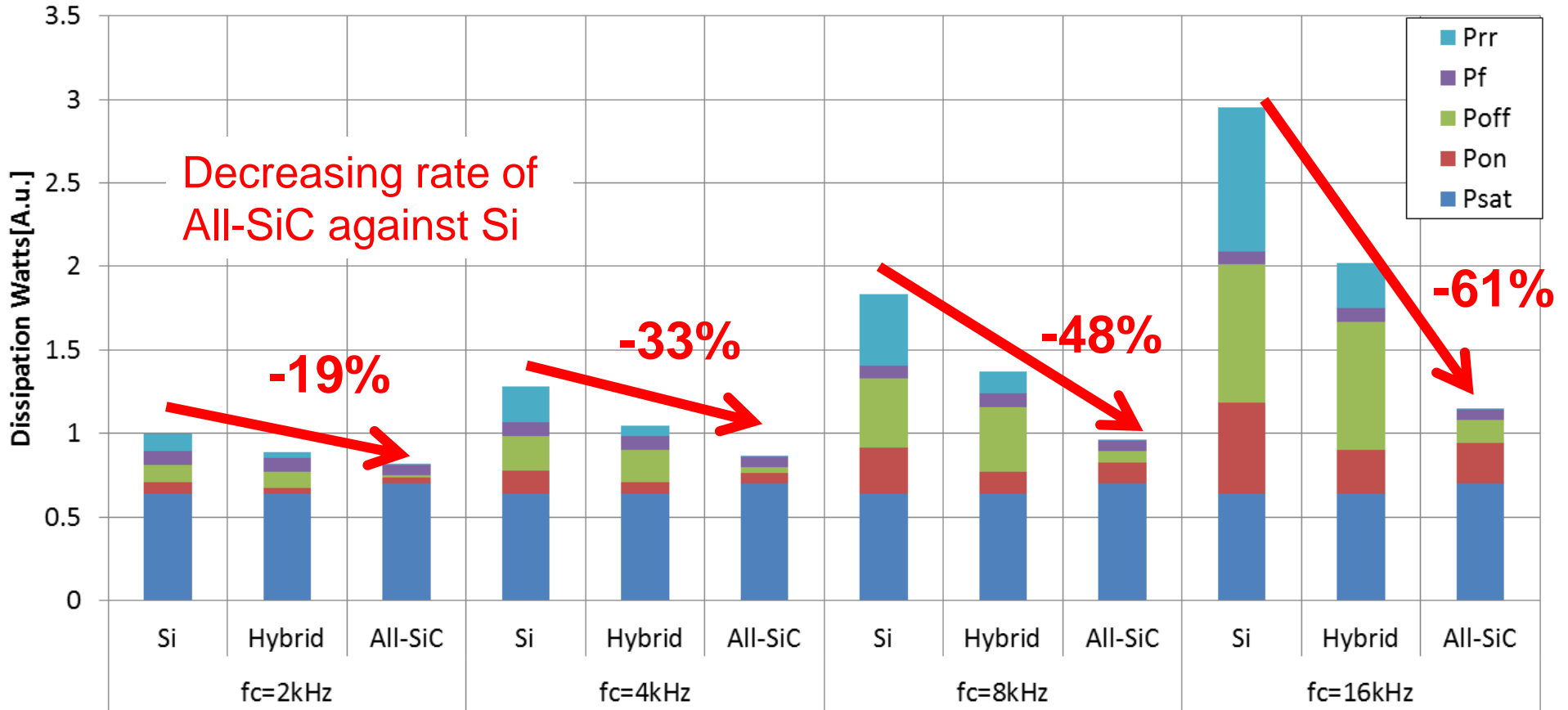
作者授权中国电源学会发布，未经作者同意禁止转载

Loss Comparison IGBT/Hybrid-SiC/All-SiC Fuji Electric *Innovating Energy Technology*

[Calc. condition]

$f_c=2 \sim 16\text{kHz}$, $V_{cc}=600\text{V}$, $I_o=1/2\text{rated}$, $\lambda=1.0$, $f_o=50\text{Hz}$, $\cos\Phi=0.9$

1200V Device



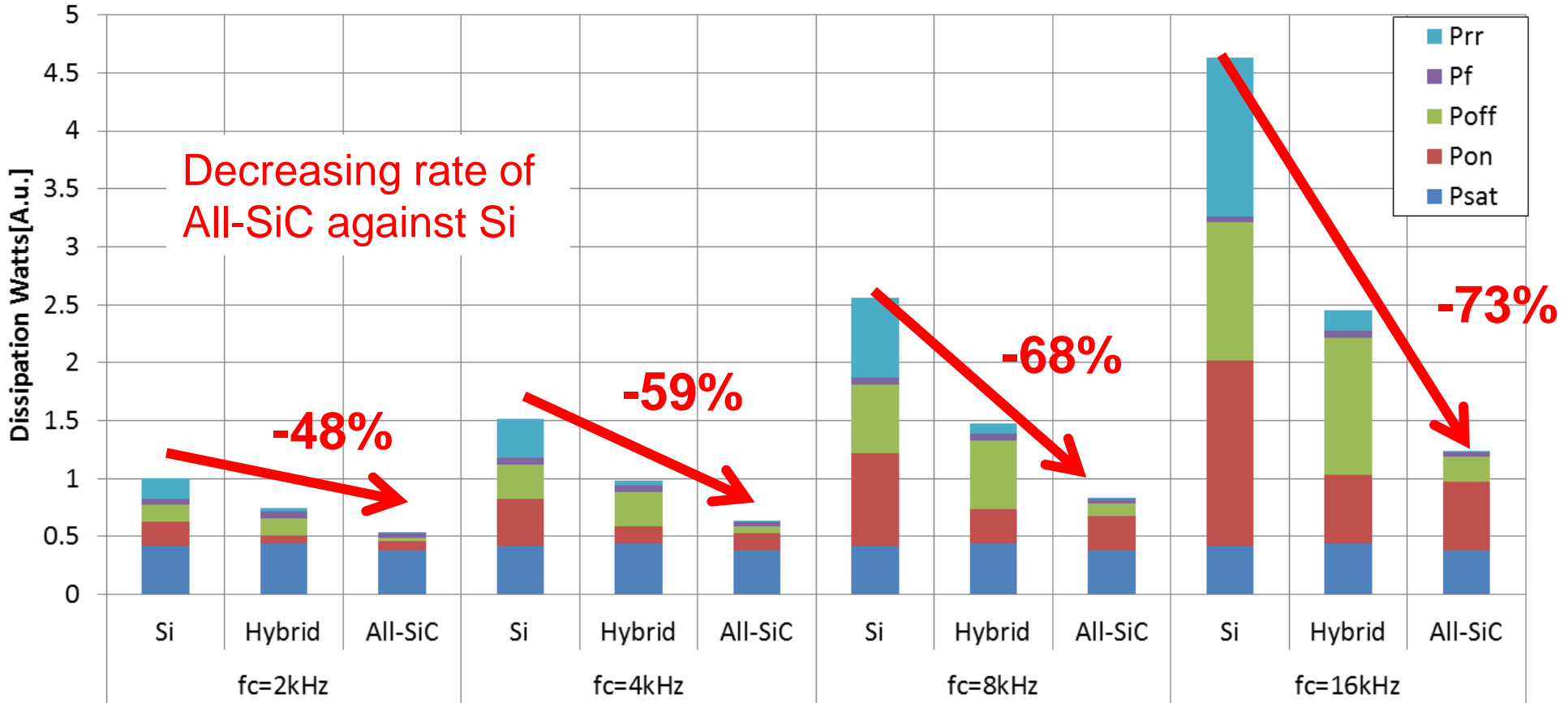
作者授权中国电源学会发布，未经作者同意禁止转载

Loss Comparison IGBT/Hybrid-SiC/All-SiC Fuji Electric *Innovating Energy Technology*

[Calc. condition]

$f_c=2 \sim 16\text{kHz}$, $V_{cc}=900\text{V}$, $I_o=1/2\text{rated}$, $\lambda=1.0$, $f_o=50\text{Hz}$, $\cos\Phi=0.9$

1700V Device



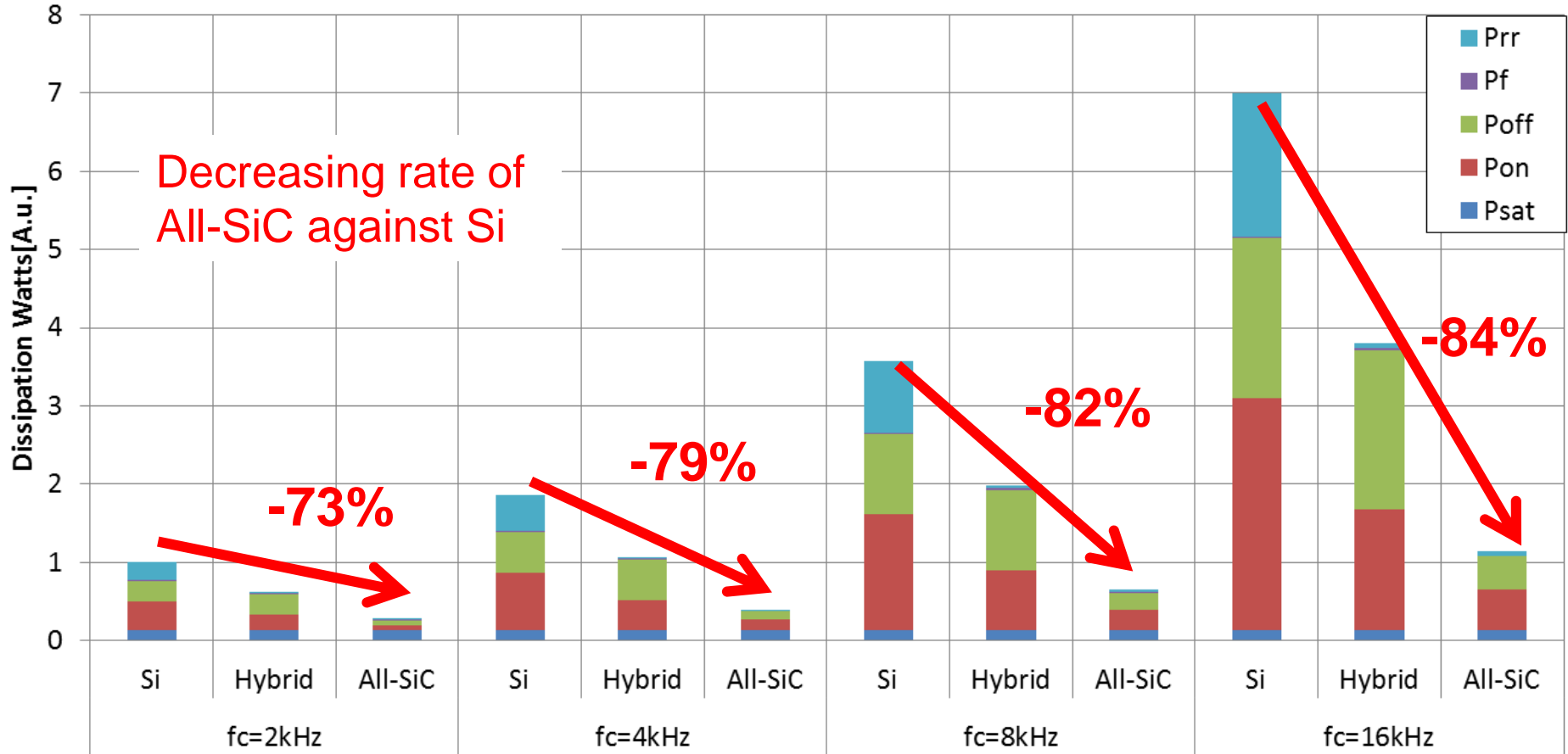
作者授权中国电源学会发布，未经作者同意禁止转载

Loss Comparison IGBT/Hybrid-SiC/All-SiC Fuji Electric *Innovating Energy Technology*

[Calc. condition]

$f_c=2 \sim 16\text{kHz}$, $V_{cc}=1800\text{V}$, $I_o=1/2\text{rated}$, $\lambda=1.0$, $f_o=50\text{Hz}$, $\cos\Phi=0.9$

3300V Device

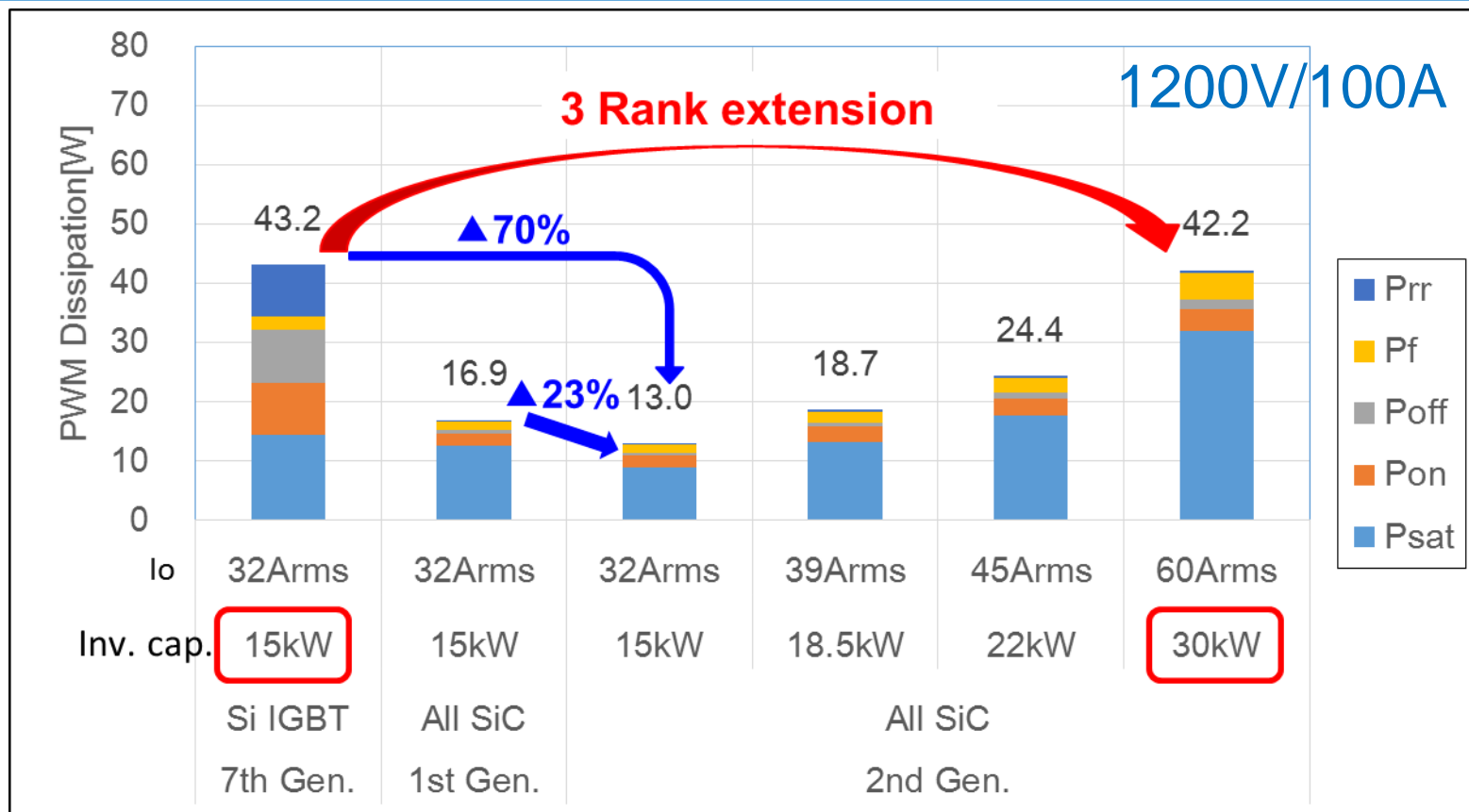


作者授权中国电源学会发布，未经作者同意禁止转载

□ SiC-MOSFET

作者授权中国电源学会发布，未经作者同意禁止转载

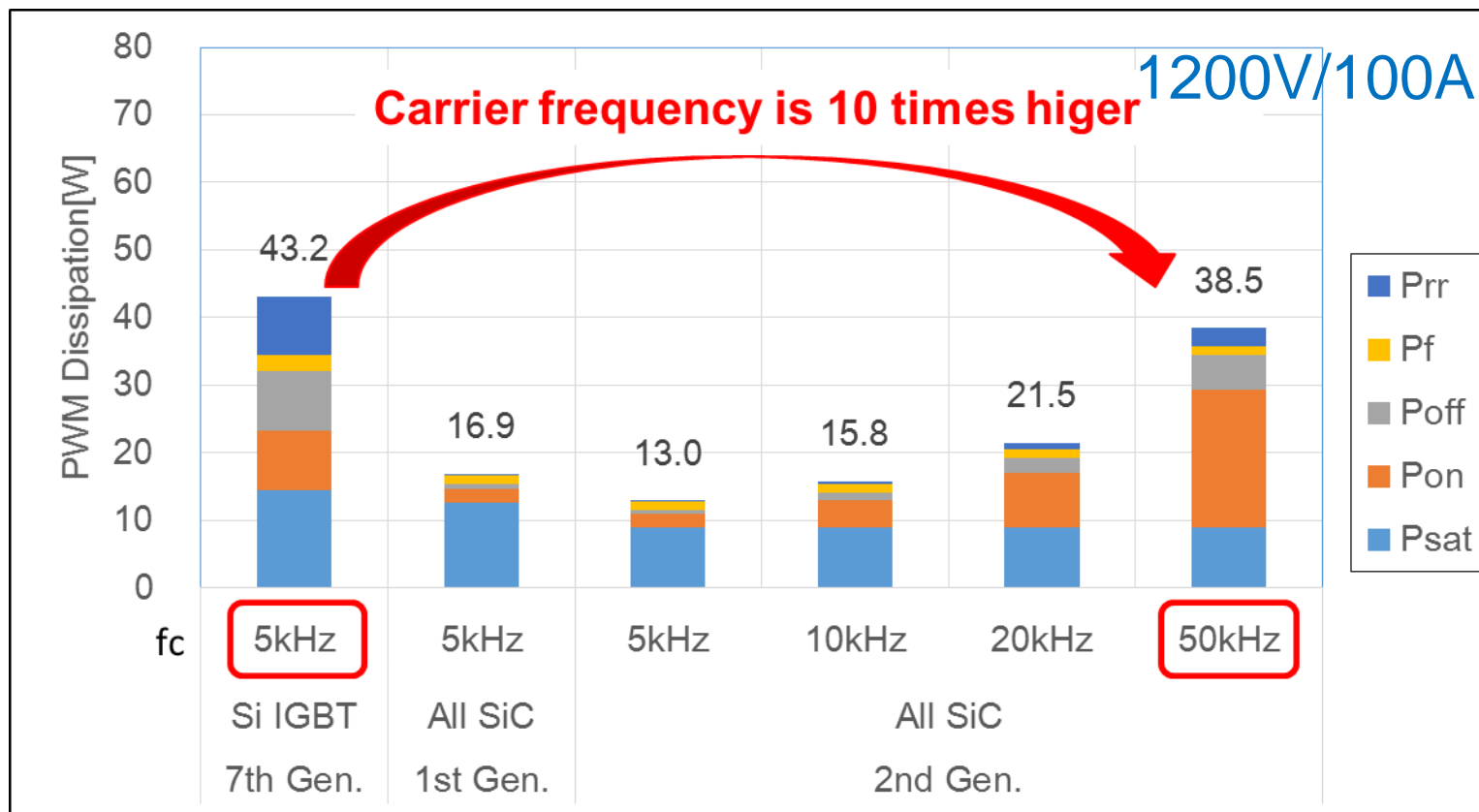
Electrical performance of All-SiC Module



The I_o for the All-SiC module was raised from **32Arms** to **60Arms** under conditions that f_c is 5 kHz, the dissipation loss was almost the same compared to 7th generation Si IGBT module.

作者授权中国电源学会发布，未经作者同意禁止转载
→ 3 rank extension for inverter capacity can be realized by applying All-SiC module.

Electrical performance of All-SiC Module



The f_c for the All-SiC module was raised from f_c 5kHz to f_c 50kHz under conditions that I_o is 32 Arms, the dissipation loss was almost the same compared to 7th generation Si IGBT module.

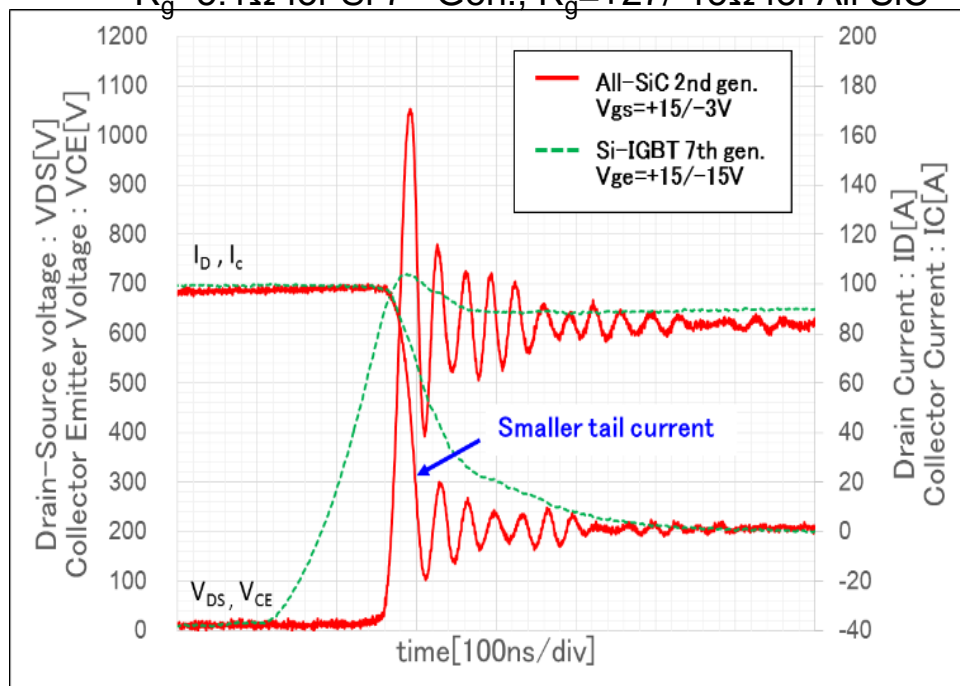
作者授权中国电源学会发布，未经作者同意禁止转载
→ 10times higher frequency can be realized by applying All-SiC module.

Switching waveforms (1200V/100A)

Turn-off waveforms

[conditions] $V_{cc}=600V$, $I_D=100A$,

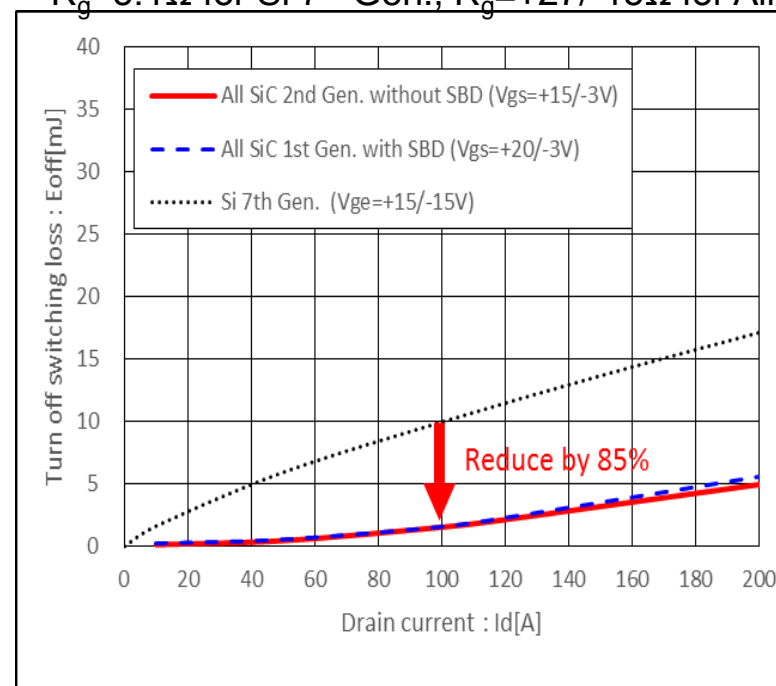
$R_g=5.1\Omega$ for Si 7th Gen., $R_g=+27/-15\Omega$ for All SiC



Turn-off switching loss with Drain current

[conditions] $V_{cc}=600V$,

$R_g=5.1\Omega$ for Si 7th Gen., $R_g=+27/-15\Omega$ for All SiC



The tail current of all-SiC module was reduced and the rising voltage was also faster compared to 7th generation Si IGBT module.

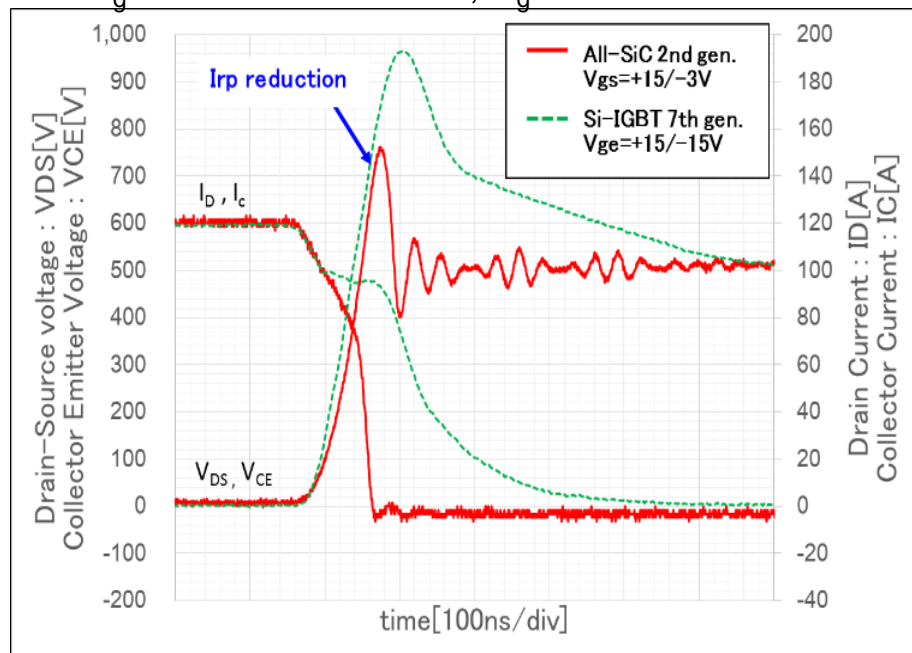
作者授权中国电源学会发布，未经作者同意禁止转载
→ Eoff was reduced by 85%.

Switching waveforms (1200V/100A)

Turn-on waveforms

[conditions] $V_{cc}=600V$, $I_D=100A$,

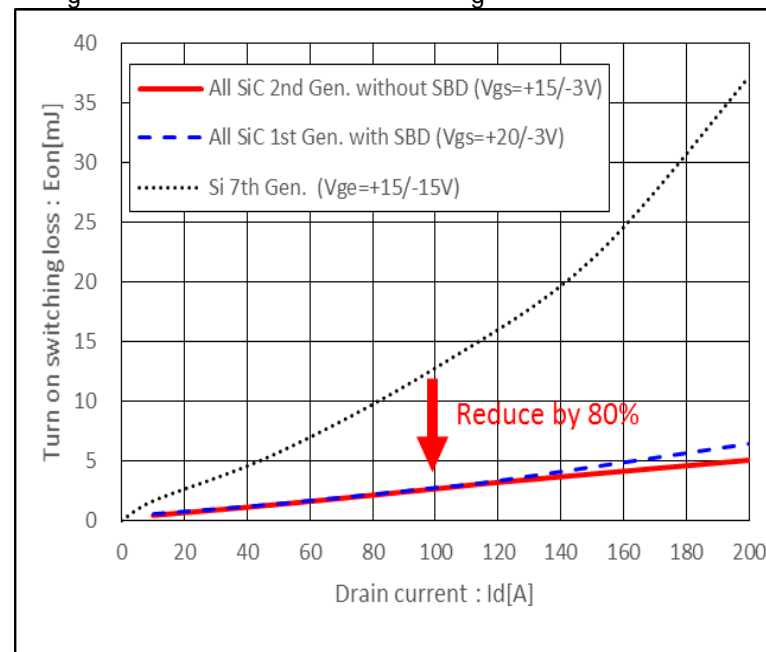
$R_g=5.1\Omega$ for Si 7th Gen., $R_g=+27/-15\Omega$ for All SiC



Turn-on switching loss with Drain current

[conditions] $V_{cc}=600V$,

$R_g=5.1\Omega$ for Si 7th Gen., $R_g=+27/-15\Omega$ for All SiC



The peak current at turn on of the all-SiC module was reduced compared to 7th generation Si IGBT module.

→ Eon was reduced by 80%.

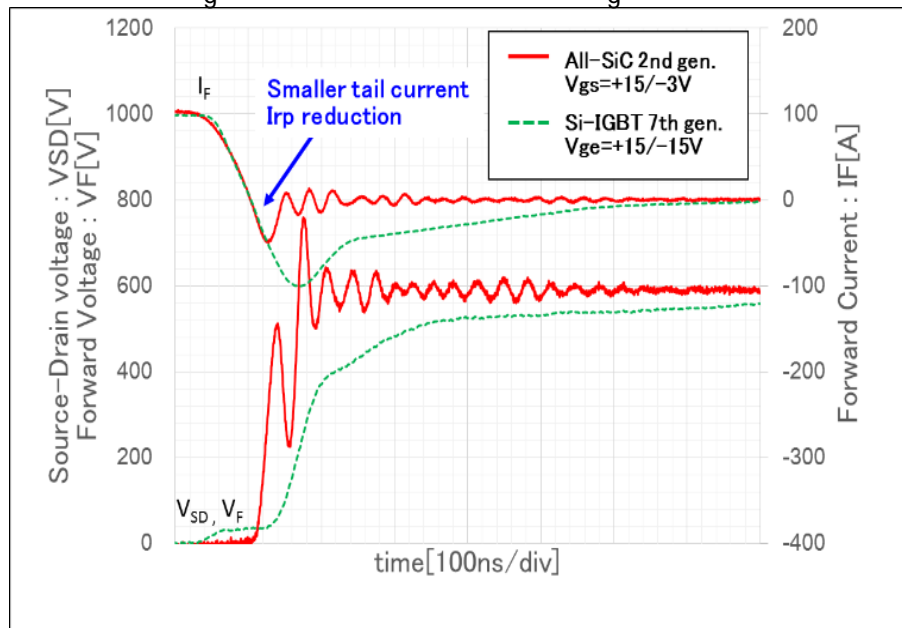
作者授权中国电源学会发布，未经作者同意禁止转载

Switching waveforms (1200V/100A) Reverse recovery switching loss

Reverse recovery waveforms

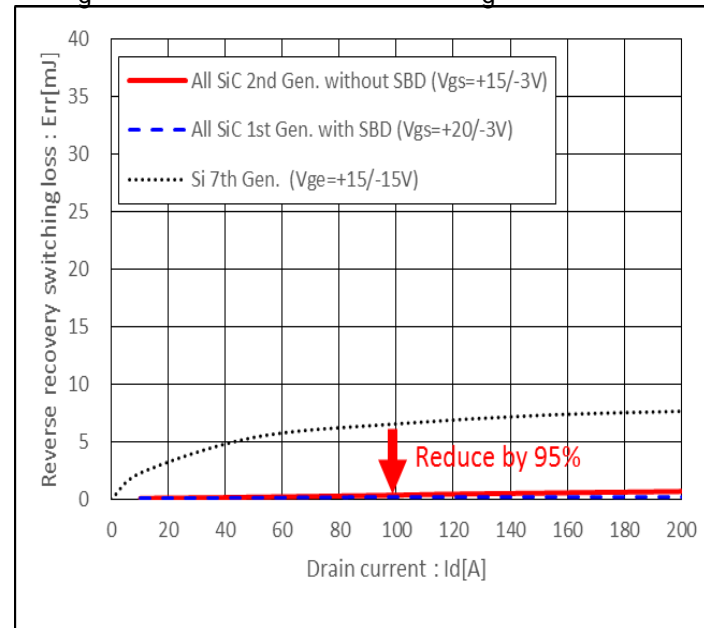
[conditions] $V_{cc}=600V$, $I_D=100A$,

$R_g=5.1\Omega$ for Si 7th Gen., $R_g=+27/-15\Omega$ for All SiC



with Drain current

[conditions] $V_{cc}=600V$,



The tail current of all-SiC module was reduced compared to the 7th generation Si IGBT module.

作者授权中国电源学会发布，未经作者同意禁止转载

Comparison of switching losses (1200V/100A)

[conditions] $V_{cc}=600V$, $I_D=100A$, $T_{vj}=175deg.C$

$R_g=5.1\Omega$, $V_{gs}=\pm 15V$ for Si 7th Gen., $R_g=+27/-15\Omega$, $V_{gs}=+15/-5V$ for All SiC

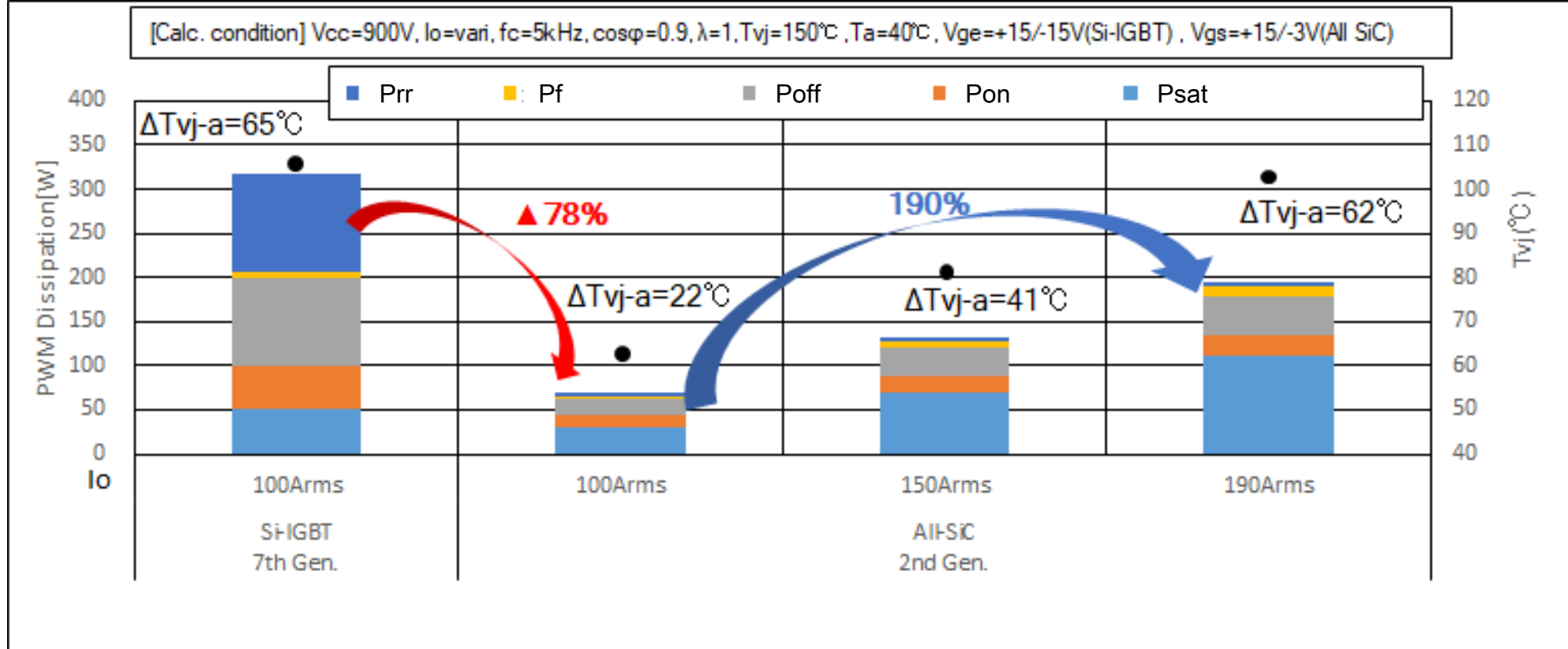
	E_{on} [mJ/pulse]	E_{off} [mJ/pulse]	E_{rr} [mJ/pulse]	E_{SW_total} [mJ/pulse]
All-SiC	2.7	1.5	0.4	4.5
7G-IGBT	12.8	9.9	6.5	29.2
Reduction rate	79%	85%	95%	85%

Total switching loss (E_{sw_total}) was dramatically reduced by 85% compared to 7th generation Si module.

→Reduction of switching loss for the inverter is expected.

作者授权中国电源学会发布，未经作者同意禁止转载

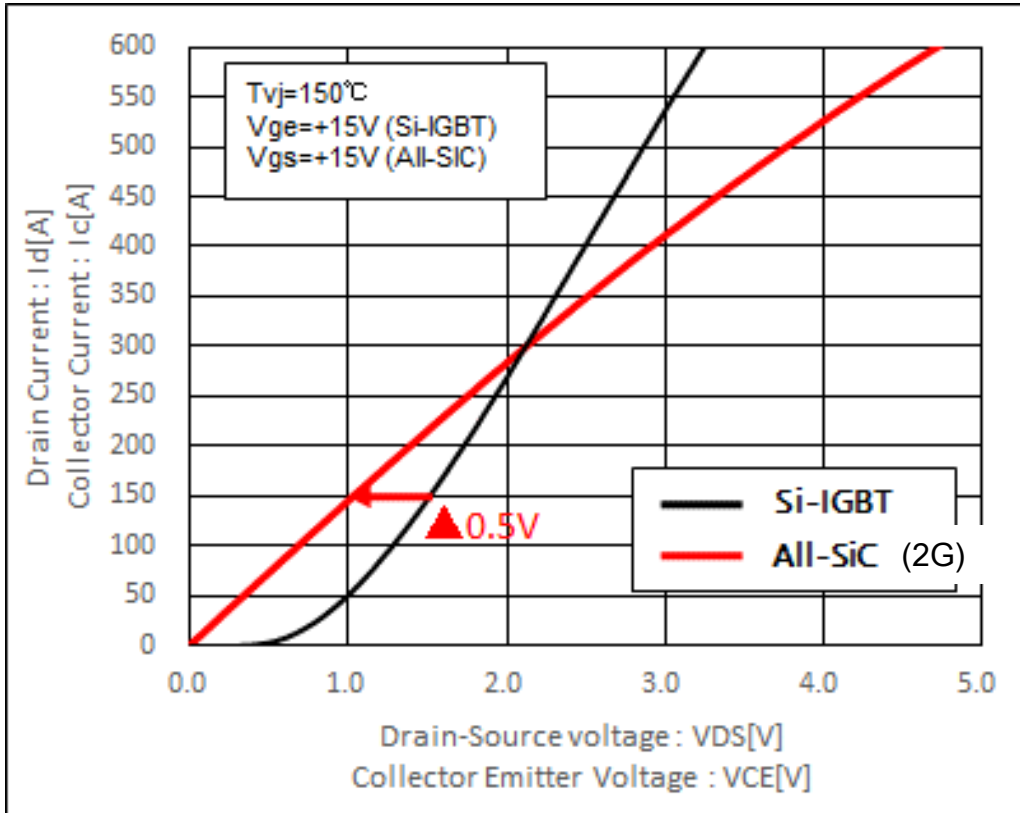
Output current of 1700V/300A All-SiC Module



The I_o for the All-SiC module was raised from 100Arms to 190Arms under conditions that f_c is 5 kHz, the dissipation loss was almost the same compared to 7th generation Si IGBT module.

→ Extension for inverter capacity can be realized by applying All-SiC module.

Si 7th Gen./All-SiC 2nd Gen. output characteristic



All-SiC output characteristic was improved!

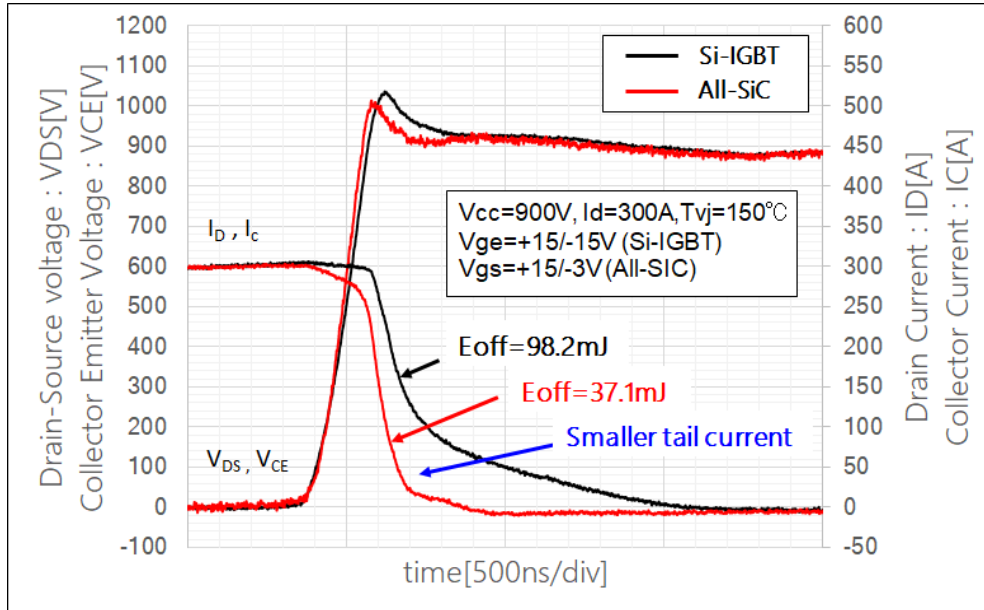
→ The on-state voltage of all-SiC module was reduced under 300A.

作者授权中国电源学会发布，未经作者同意禁止转载

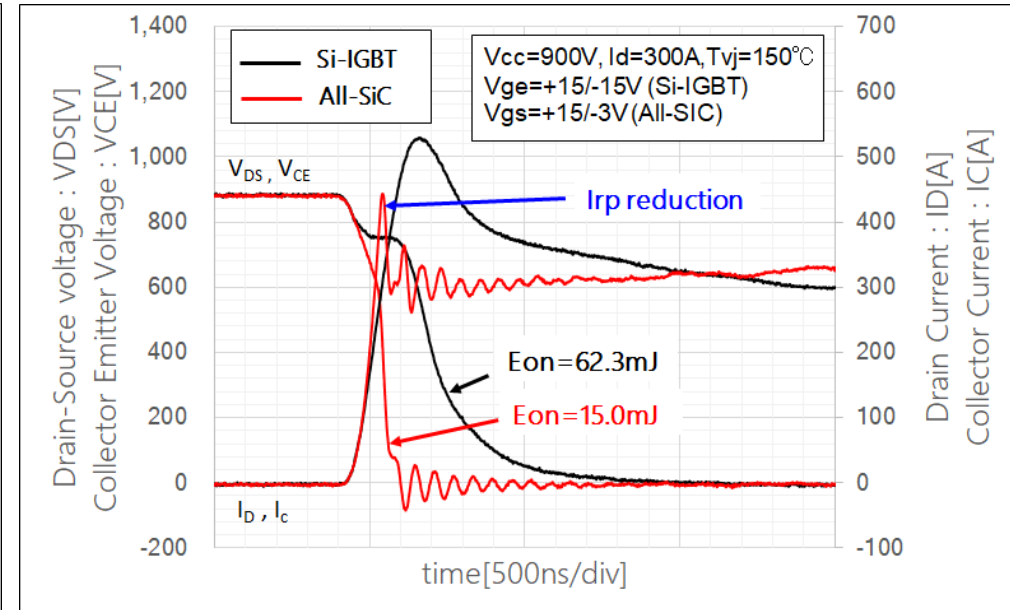
[conditions] $V_{cc}=900V$, $I_D=300A$, $T_{vj}=150^{\circ}C$

$V_{ge}=+15/-15V$ (Si-IGBT), $V_{gs}=+15/-3V$ (All-SiC)

Turn-off waveforms



Turn-on waveforms



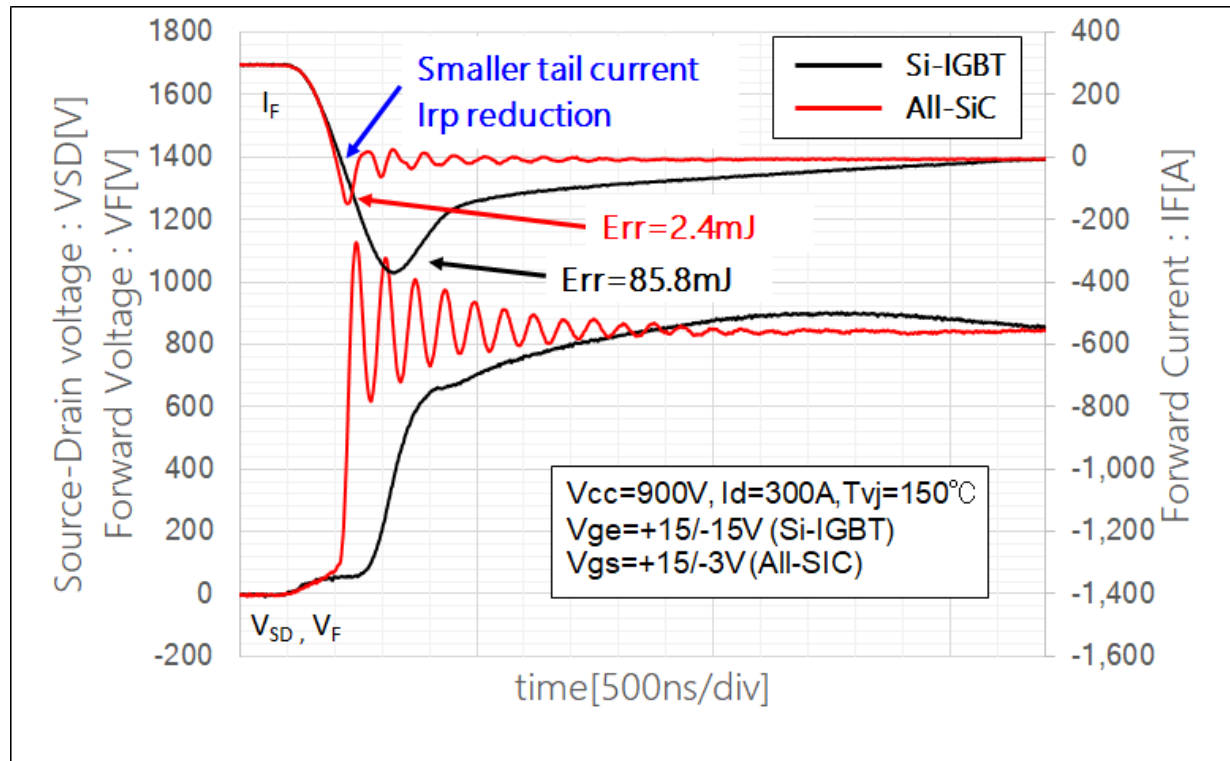
The tail current of all-SiC module was reduced and the rising voltage was also faster compared to 7th generation Si IGBT module.

→ E_{off} was reduced by 62%.

The peak current at turn on of the all-SiC module was reduced compared to 7th generation Si IGBT module.

→ E_{on} was reduced by 76%.

[conditions] $V_{CC}=900V$, $I_D=300A$, $T_{vj}=150^{\circ}C$



The tail current of all-SiC module was reduced compared to the 7th generation Si IGBT module.

作者授权中国电源学会发布，未经作者同意禁止转载

[conditions] $V_{cc}=900V$, $I_D=300A$, $T_{vj}=150deg.C$
 $V_{ge}=\pm 15V$ for Si-IGBT, $V_{gs}=+15/-3V$ for All SiC

	Eon [mJ/pulse]	Eoff [mJ/pulse]	Err [mJ/pulse]	Esw_total [mJ/pulse]
All-SiC (2G)	15.0	37.1	2.4	54.5
7G-IGBT	62.3	98.2	85.8	246.3
Reduction Rate	76%	62%	97%	78%

Total switching loss (Esw_total) was dramatically reduced by 78% compared to 7th generation Si module.

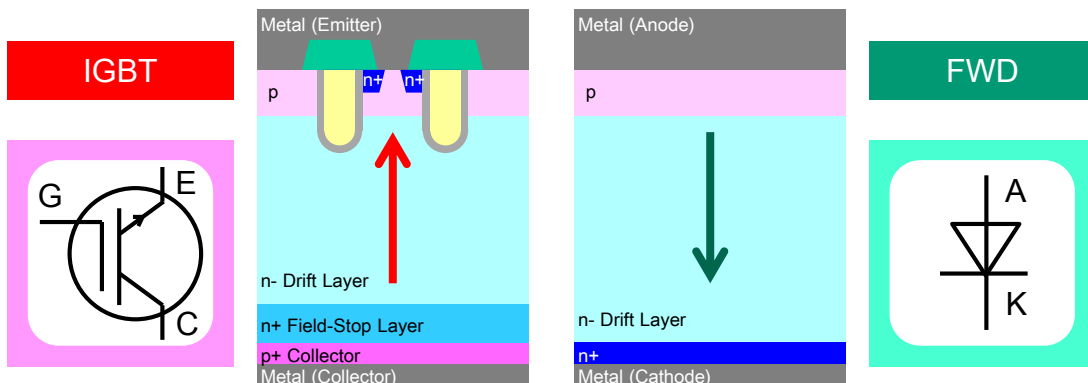
→Reduction of switching loss for the inverter is expected.

作者授权中国电源学会发布，未经作者同意禁止转载

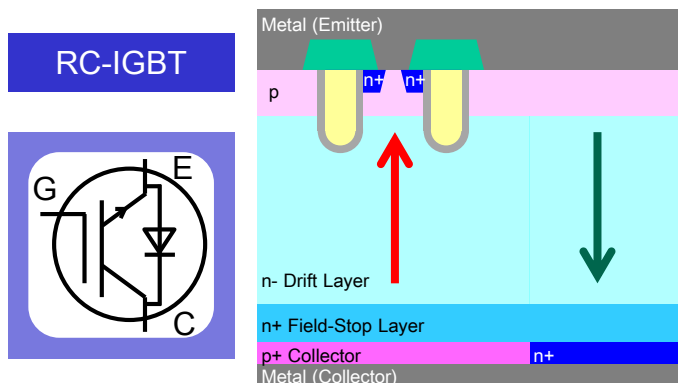
□ RC-IGBT for Wind Turbine

作者授权中国电源学会发布，未经作者同意禁止转载

RC-IGBT Chip Structure



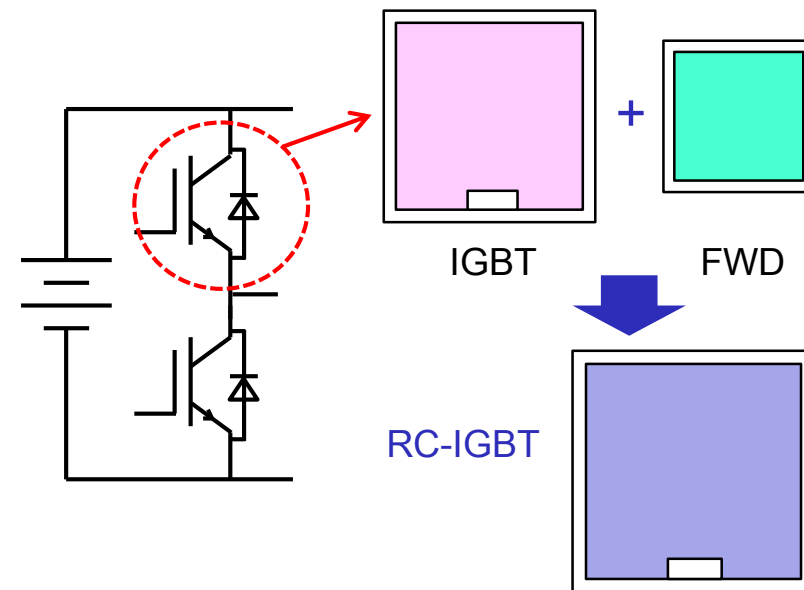
Integrating IGBT and FWD into one chip



Basic Structure of RC-IGBT

- Based on the X Series IGBT/FWD technology

RC-IGBT Chip and Circuit Diagram

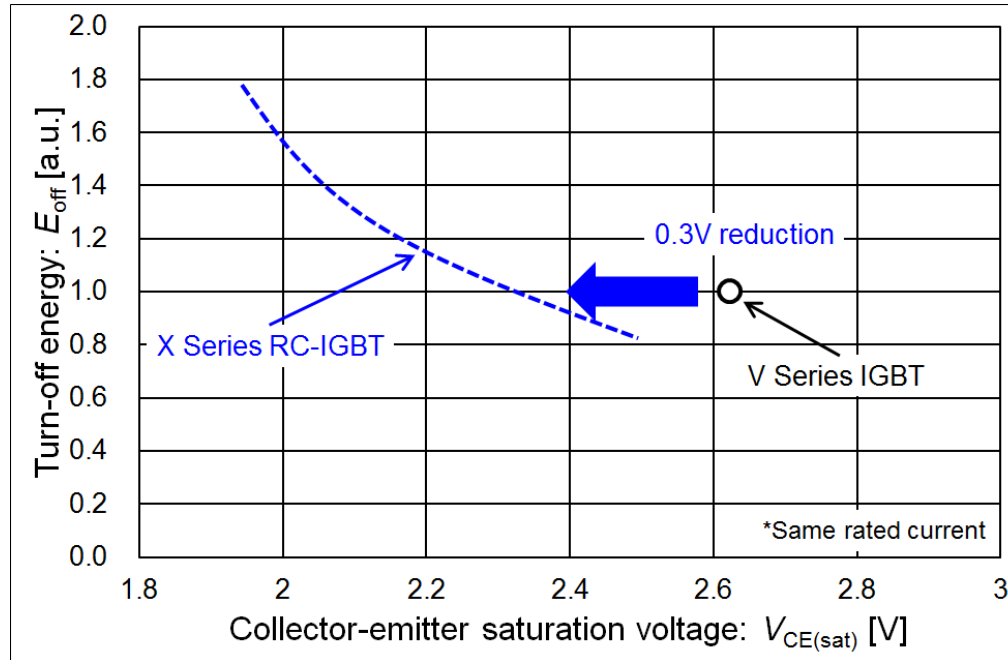


Advantage of RC-IGBT

- Total chip size reduction
 - Downsizing of the Module or High current rating with existing package
- Extending chip area
 - Chip Temperature reduction by Lower $R_{th(j-c)}$

c)

1,700V X Series RC-IGBT trade-off relationship between $V_{CE(sat)}$ and E_{off}



Measurement conditions:

$V_{CE(sat)}$: $T_{vj}=150^{\circ}\text{C}$, $V_{GE}=+15\text{V}$, $I_C=\text{rated current}$

E_{off} : $T_{vj}=150^{\circ}\text{C}$, $V_{GE}=+15\text{V}/-15\text{V}$, $V_{CC}=900\text{V}$, $I_C=\text{rated current}$

■ 1,700 V X Series RC-IGBT trade-off relationship of IGBT was improved as compared with V Series IGBT.

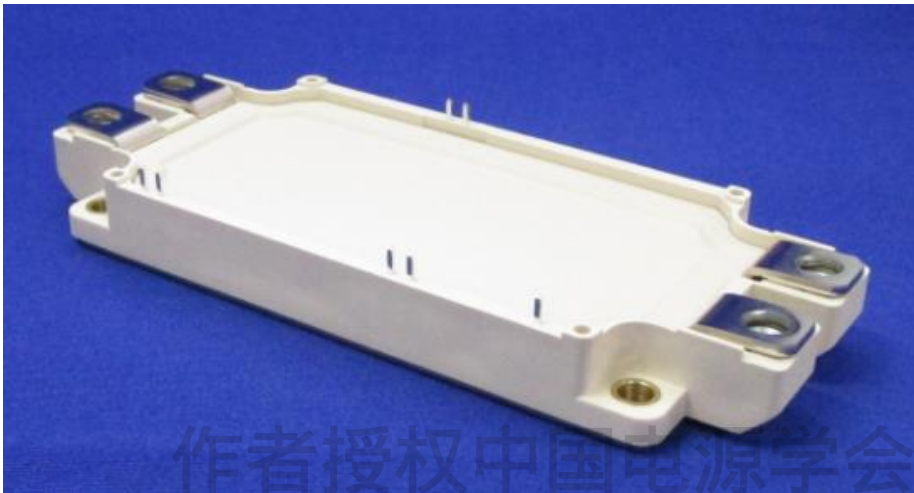
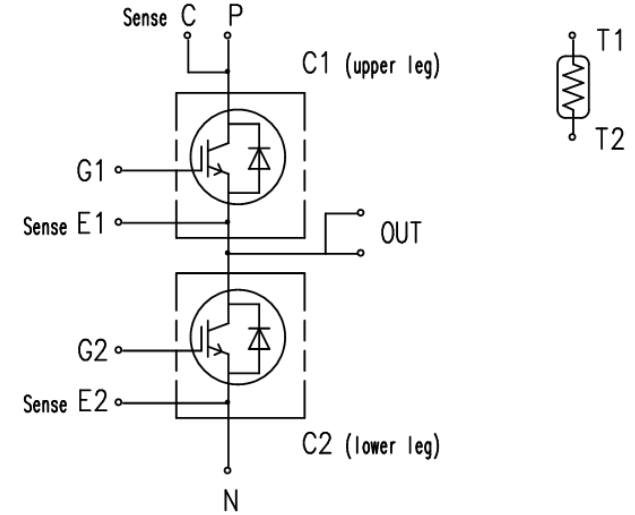
□ $V_{CE(sat)}$ improvement by 0.3V under the same E_{off} condition

作者授权中国电源学会发布，未经作者同意禁止转载

Dual XT 1700V/800A

Dual XT 1700V/800A

Type Name	2MBI800XRNE170-50 (Solder pin type)
	2MBI800XRNF170-50 (Press-fit pin type)
Rated Voltage	1,700V
Rated Current	800A
Generation	7th-Generation "X Series"
Device	X Series RC-IGBT
Package	X Series M285 (Solder pin type)
	X Series M286 (Press-fit pin type)

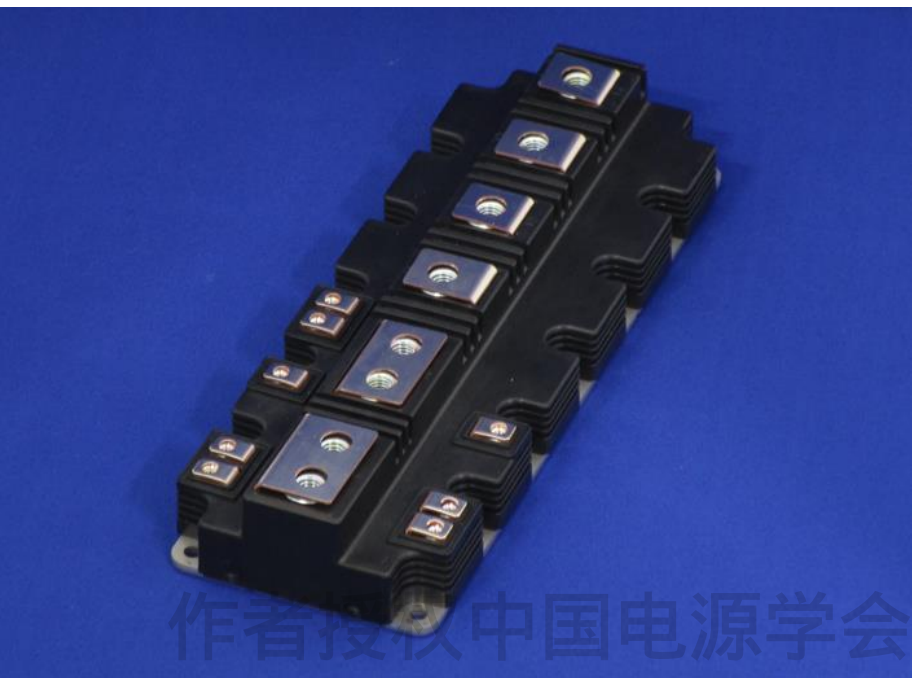
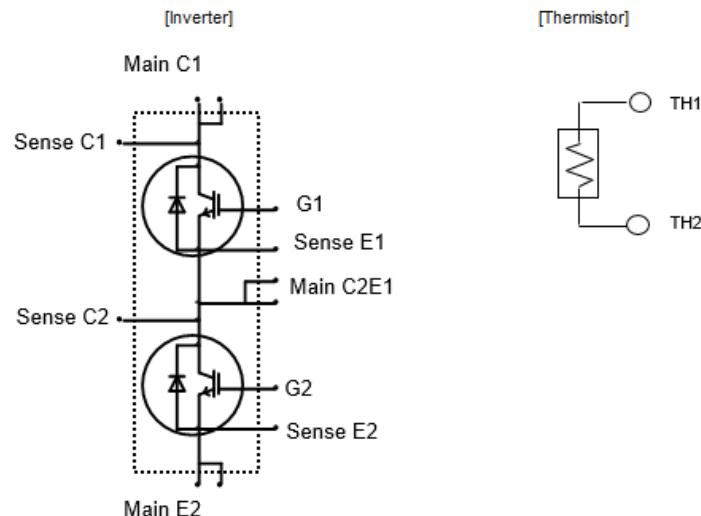


Rated Voltage	Rated Current [A]						
	1,700V	225	300	450	550	600	800
DualXT	V Series IGBT + FWD						X-RC
	X Series IGBT + FWD						★

作者授权中国电源学会发布，未经作者同意禁止转载

PrimePACK™ 3+ 1700V/2200A

Type Name	2MBI2200XRXF170-50
Rated Voltage	1,700V
Rated Current	2.200A
Generation	7th-Generation “X Series”
Device	X Series RC-IGBT
Package	X Series M291



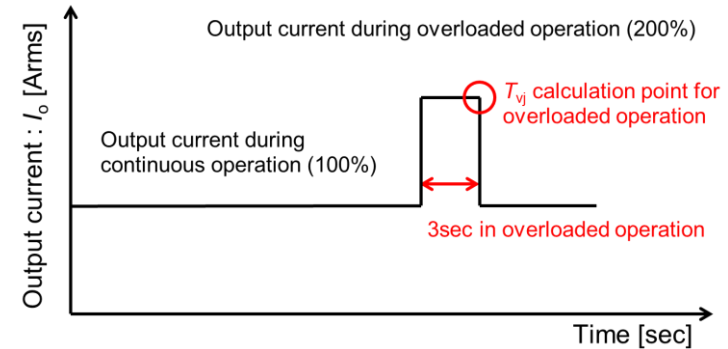
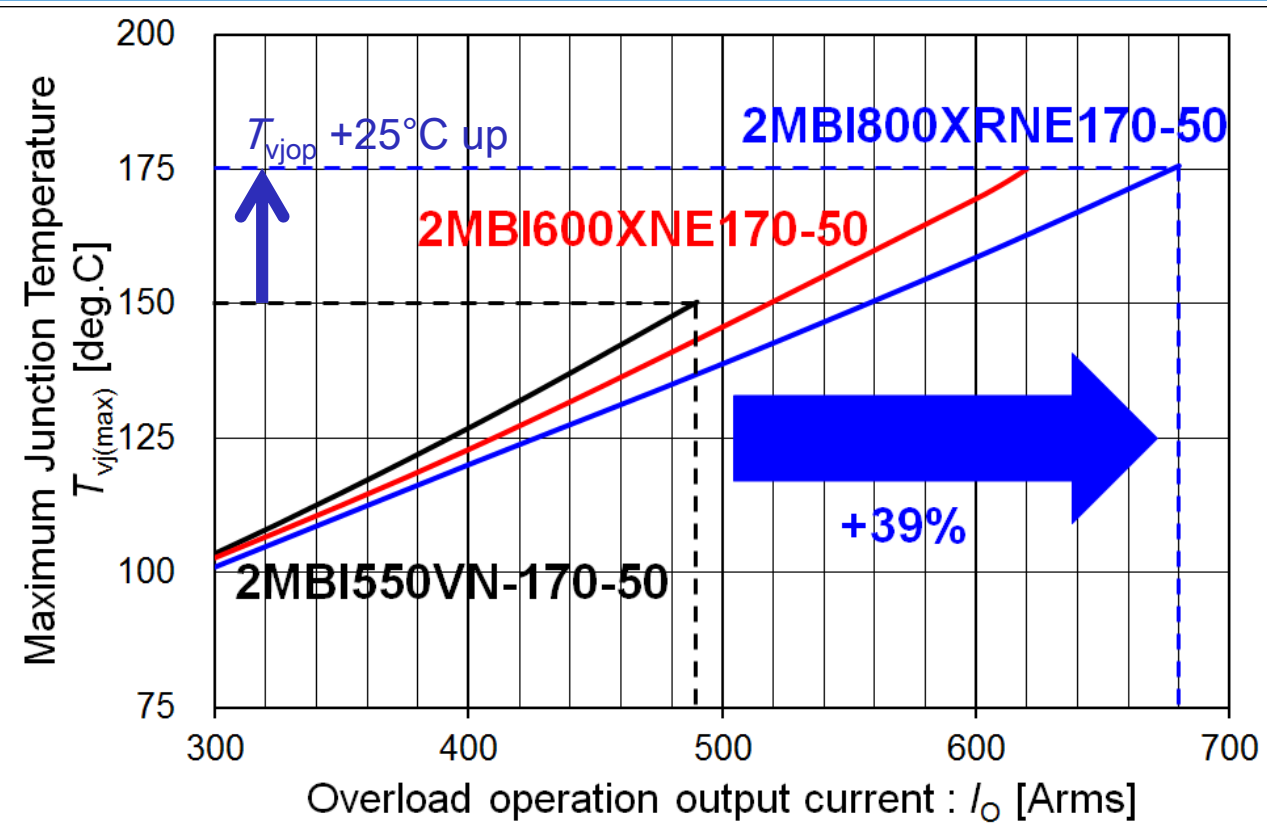
Rated Voltage	Rated Current [A]			
	1,000	1,400	1,800	2,200
PrimePACK™	V Series IGBT + FWD			X-RC
	X Series IGBT + FWD			★

Note:

PrimePACK™ is registered trademark of Infineon Technologies AG, Germany, 未经作者同意禁止转载

Calculation results for relationship between T_{vj} and I_o

(under the overload operation condition)



Calculation conditions:
 $T_{vj}=150\text{deg.C}$, $V_{CC}=900\text{V}$, $f_o=50\text{Hz}$, $f_c=2\text{kHz}$, Power factor=0.9, Modulation rate=1.0, Ambient temperature $T_a=50^\circ\text{C}$, same cooling conditions

■ 1,700V X Series RC-IGBT module Dual XT has been able to expand the I_o by 39% with same package size during overload operation compared with V Series.

- Reducing the power dissipation and $R_{th(j-c)}$
- Expanding the T_{vjop} from 150deg.C to 175deg.C

作者授权中国电源学会发布，未经作者同意禁止转载

What is one of major application for 1,700 V IGBT modules?

■ Wind power generation systems

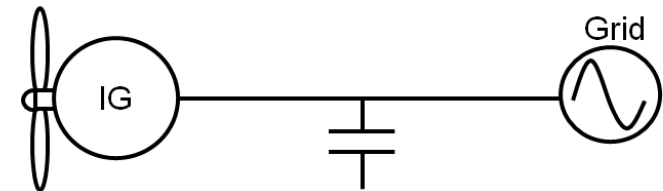
DFIG and BTB systems utilize power conversions.

■ DFIG

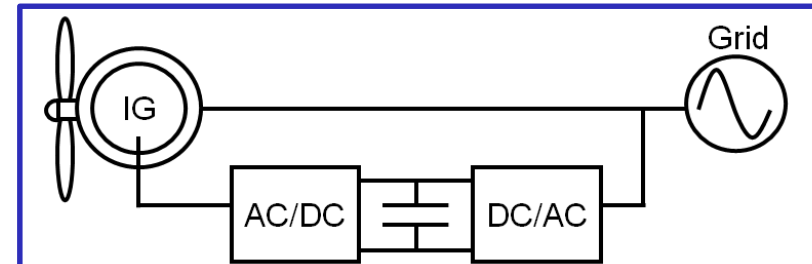
Power converter is connected to the rotor to control the rotor frequency and current.
The converter size is around 30% of the system.

■ BTB

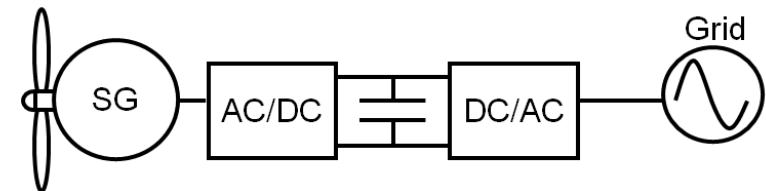
Power converter controls full power and full speed range of the system.



(a) Induction Generator: IG

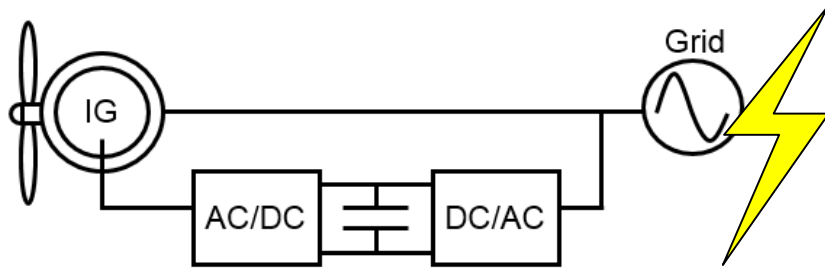


(b) Doubly-Fed Induction Generator: DFIG



(c) Full-scale Back-To-Back converter: BTB

Instantaneous voltage drop

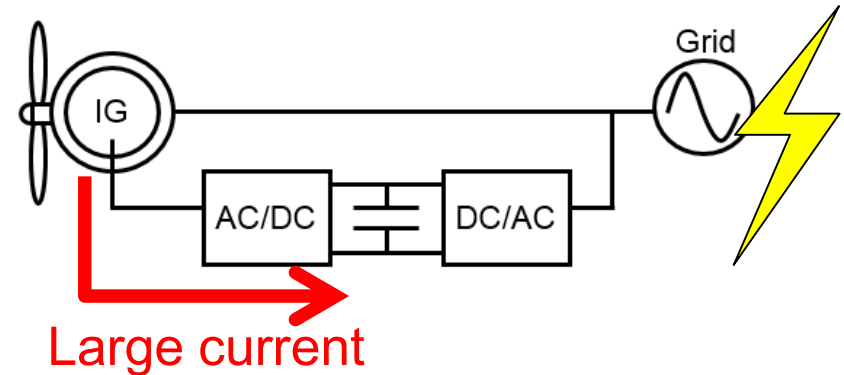


Instantaneous voltage drop occurs in the grid...

- The system will stop.
- There is the risk of instability to the grid.

- The operation continuous function (LVRT) becomes important to supply the stable power to the grid.

LVRT operation



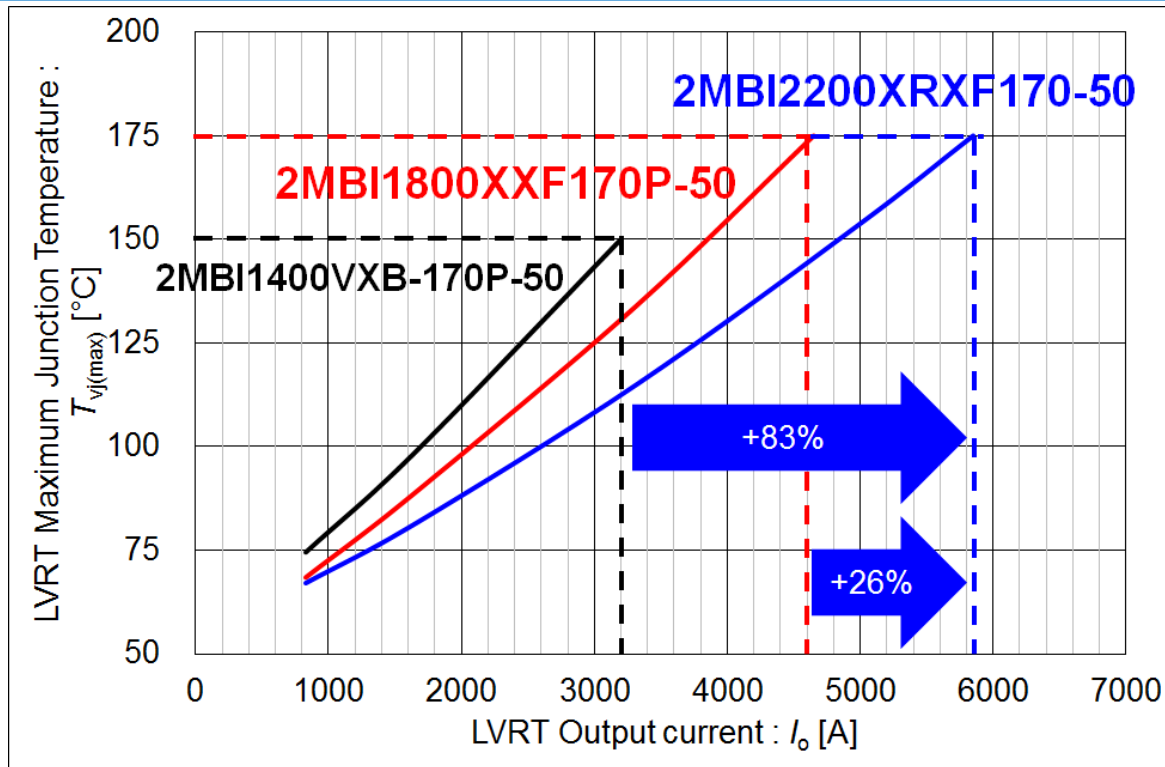
In case of the LVRT operation...

- Large current will flow from generator to the capacitor through the FWD of rotor side.

- Large current capability of FWD is important.

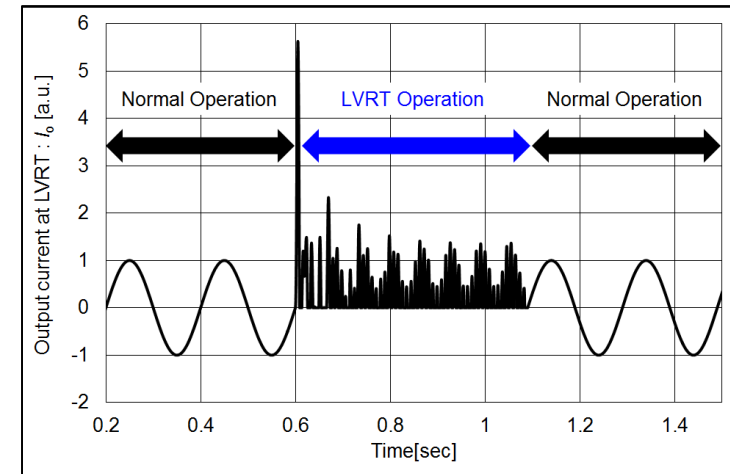
作者授权中国电源学会发布，未经作者同意禁止转载

Calculation results for relationship between T_{vj} and I_o (under the LVRT operation condition)



Calculation conditions:

T_{vj} =150deg.C, V_{cc} =1100V, f_o =1.5Hz, f_c =2.5kHz, Power factor=-0.65, Modulation rate=0.15, Ambient temperature T_a =50°C, same cooling conditions

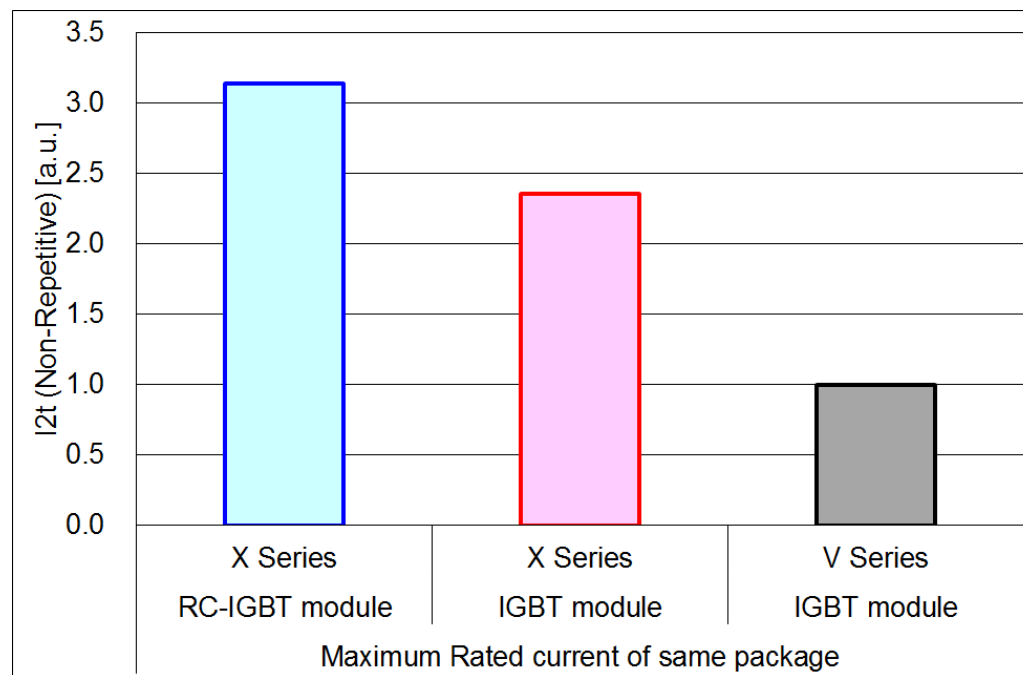


■ 1,700V X Series RC-IGBT module PrimePACK™ has been able to expand the I_o by 83% with same package size during overload operation compared with V Series.

- In X Series RC-IGBT, IGBT and FWD regions are optimized.
- The temperature balance inside the device is optimized.
- Therefore, the thermal resistance and large current capability are improved.

Note: PrimePACK™ is registered trademark of Infineon Technologies AG, Germany

© Fuji Electric Co., Ltd. All rights reserved.



Measurement conditions:
 $T_{vj}=150\text{deg.C}$, $t=10\text{ms}$ (Half sine wave form), Non-Repetitive

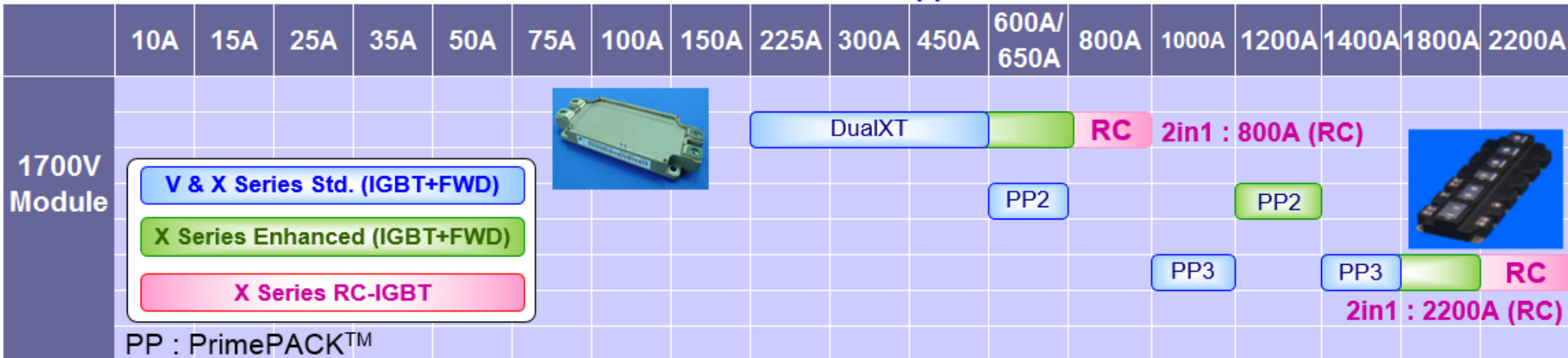
- 1,700 V X Series RC-IGBT module has increased over 200% I^2t capability compared with conventional V Series.
- IGBT region becomes buffer layer of heat during the FWD operation, which is the reason of high I^2t capability.

作者授权中国电源学会发布，未经作者同意禁止转载

Product Line-up of 1,700 V X Series RC-IGBT Modules

- X Series RC-IGBT Modules can achieve more enhancement & downsizing.
- X Series IGBT Module family will be expanded for premium range by X Series RC-IGBT.

1700V 7th-Generation "X Series" RC-IGBT Modules for Industrial Application



Note: PrimePACK™ is Trademark or registered trademark of Infineon Technologies AG, Germany

作者授权中国电源学会发布，未经作者同意禁止转载